Plant Biotechnology Journal
Open Access

Plant Biotechnology Journal (2022) **20**, pp. 2389–2405 doi: 10.1111/pbi.13920

CC-type glutaredoxin, MeGRXC3, associates with catalases and negatively regulates drought tolerance in cassava (*Manihot esculenta* Crantz)

Xin Guo[1,2,†], Xiaoling Yu[1,2,†], Ziyin Xu[3], Pingjuan Zhao[1,2], Liangping Zou[1,2], Wenbin Li[1,2], Mengting Geng[3], Peng Zhang[4], Ming Peng[1,2] and Mengbin Ruan[1,2,*]

[1]*Key Laboratory of Biology and Genetic Resources of Tropical Crops, Institute of Tropical Bioscience and Biotechnology, Chinese Academy of Tropical Agricultural Sciences, Haikou, China*

[2]*Hainan Key Laboratory for Protection and Utilization of Tropical Bioresources, Hainan Institute for Tropical Agricultural Resources, Haikou, China*

[3]*College of Tropical Crops, Hainan University, Haikou, China*

[4]*National Key Laboratory of Plant Molecular Genetics, CAS Center for Excellence in Molecular Plant Sciences, Shanghai Institutes for Biological Sciences, Chinese Academy of Sciences, Shanghai, China*

Received 31 May 2022;
revised 5 August 2022;
accepted 27 August 2022.
**Correspondence* (Tel +86-898-66987892; fax +86-898-66890978; email ruanmengbin@itbb.org.cn)
[†]These authors contributed equally.

Keywords: Cassava (*Manihot esculenta* Crantz), catalase, CC-type glutaredoxin, drought tolerance, ROS homeostasis, stomatal movement.

Summary

Glutaredoxins (GRXs) are essential for reactive oxygen species (ROS) homeostasis in responses of plants to environment changes. We previously identified several drought-responsive CC-type GRXs in cassava, an important tropical crop. However, how CC-type GRX regulates ROS homeostasis of cassava under drought stress remained largely unknown. Here, we report that a drought-responsive CC-type GRX, namely MeGRXC3, was associated with activity of catalase in the leaves of 100 cultivars (or unique unnamed genotypes) of cassava under drought stress. *MeGRXC3* negatively regulated drought tolerance by modulating drought- and abscisic acid-induced stomatal closure in transgenic cassava. It antagonistically regulated hydrogen peroxide (H_2O_2) accumulation in epidermal cells and guard cells. Moreover, MeGRXC3 interacted with two catalases of cassava, MeCAT1 and MeCAT2, and regulated their activity *in vivo*. Additionally, MeGRXC3 interacts with a cassava TGA transcription factor, MeTGA2, in the nucleus, and regulates the expression of *MeCAT7* through a MeTGA2-MeMYB63 pathway. Overall, we demonstrated the roles of *MeGRXC3* in regulating activity of catalase at both transcriptional and post-translational levels, therefore involving in ROS homeostasis and stomatal movement in responses of cassava to drought stress. Our study provides the first insights into how MeGRXC3 may be used in molecular breeding of cassava crops.

Introduction

Drought stress negatively affects plant growth and development and can, therefore reduce agricultural yield (Boyer, 1982). However, many plants have developed stress response mechanisms to adapt their patterns of growth under drought stress (Claeys and Inze, 2013). One such plant is cassava (*Manihot esculenta* Crantz), which is the most important staple crop in many tropical and subtropical arid regions of the world that are characterized by alternating wet and prolonged drought periods. These regions include sub-Saharan Africa, subtropical Asia and parts of South America (Hillocks *et al.*, 2002). To support robust drought tolerance in cassava, many cultivars have been developed with differing drought response strategies, such as quick stomatal closure, reduction in photosynthetic proteins levels and photosynthetic capacity, induction of senescence in older leaves and size reduction in epidermal cells of leaves (Alves and Setter, 2004; Zhao *et al.*, 2014). However, drought still seriously affects growth and tuber roots formation of cassava cultivars at seedling stage (Kengkanna *et al.*, 2019). Recently, many drought-responsive genes in cassava have been identified via high-throughput sequencing methods (Ding *et al.*, 2019b; Ruan *et al.*, 2017, 2018; Suksamran *et al.*, 2020; Weng *et al.*, 2021), but only few of these have been analysed. Therefore, the genomic mechanism by which cassava is adapted to drought, especially through human-mediated selection, remained largely unknown.

A prior study (Xu *et al.*, 2013a) showed that drought tolerance in cassava improved under the combined expression of SOD (Cu/Zn-superoxide dismutase) and CAT (catalase), which are enzymatic scavengers of reactive oxygen species (ROS) that become more abundant during drought stress and caused damage to plant cells (Wrzaczek *et al.*, 2013). Moreover, drought-induced leaf abscission in cassava was delayed in transgenic cassava overexpressing SOD and CAT (Liao *et al.*, 2016), while a heat shock protein, MeHSP90, was found to recruit MeWRKY20 and MeCAT1 to regulate drought-induced ROS accumulation in leaves of a casava cultivar (Wei *et al.*, 2020). In addition, a transcription factor, MeRAV5, interacts with peroxidase (POD), which negatively regulates ROS accumulation under drought stress (Yan *et al.*, 2021a). Silencing *MeRAV5* by in leaves virus-induced gene silence yielded drought sensitivity in a cassava cultivar (Yan *et al.*, 2021a). Taken together, these studies highlight the importance of mitigation of ROS activities and

maintenance of their homeostasis in cassava during drought stress.

The glutathione/glutaredoxin (GSH/GRX) system is essential for ROS signalling and protein redox homeostasis in responses of plants to stress (Meyer *et al.,* 2012). GRXs are classified into five subgroups. The CC-type is specific to land plants and was characterized as the ROXY family in *Arabidopsis* (Meyer *et al.,* 2012). In *Arabidopsis*, overexpression of *ROXY1* was correlated with a significant increase in ROS accumulation and caused higher susceptibility to fungal infection by *Botrytis* E. M. Fries, 1832 (Wang *et al.,* 2009). On the contrary, the *roxy18* mutant showed higher initial and photo-oxidative stress-induced ROS accumulation, and therefore caused sensitivity to methyl viologen herbicide and high light (Laporte *et al.,* 2012). These results indicate that ROXYs play antagonistic roles in ROS homeostasis. However, how CC-type GRX regulates ROS homeostasis remained largely unknown.

Direct redox modification of transcription factors is critical for the perception of intracellular ROS (Wrzaczek *et al.,* 2013). For example, redox modification of a basic domain leucine zipper (bZIP) transcription factor, TGACG-BINDING FACTOR 1 (TGA1), affected its transcriptional regulation ability (Lindermayr *et al.,* 2010). TGA1 appears to interact with several CC-type GRXs, such as ROXY9, ROXY18 and ROXY19 (Li *et al.,* 2019). Physical interaction with ROXY19 and subsequent redox modification of TGA2 is essential for the function of this transcription factor (Zander *et al.,* 2012). Furthermore, ROXY1 and ROXY2 regulate anther development by controlling redox modification of TGA9 and TGA10 in *Arabidopsis* (Li *et al.,* 2009; Murmu *et al.,* 2010; Xing and Zachgo, 2008).

CC-type GRXs are also involved in abiotic stress and phytohormone responses in plants (Ndamukong *et al.,* 2007; Zander *et al.,* 2012). In rice, the expression of *OsGRX8* is induced by auxin and abiotic stress (Sharma *et al.,* 2013). Furthermore, overexpression of *OsGRX8* in *Arabidopsis* enhanced tolerance to abscisic acid (ABA) and abiotic stresses (Sharma *et al.,* 2013). Another CC-type GRX of rice, *OsGRX6*, undergoes changes in expression levels depending on the availability of nitrate, and overexpression of this gene delays leaf senescence and causes gibberellic acid insensitivity (El-Kereamy *et al.,* 2015). These data from model species indicate that CC-type GRXs may be useful in improving the resistance of crops to abiotic stress.

Previously, we screened several CC-type GRXs, which respond to drought and ABA in cassava cultivars (Ruan *et al.,* 2018). For one gene, *MeGRXC3*, we determined that its overexpression cause mannitol-induced osmotic stress sensitivity in transgenic *Arabidopsis* (Ruan *et al.,* 2022). However, whether MeGRXC3 is involved in ROS signalling and drought resistance in cassava remains unclear. Here, we found that two SNPs in the promoter of *MeGRXC3* are significantly associated with the activity of catalase in mature leaves of 100 cultivars of cassava (or unnamed or informally named genotypes; hereafter cultivars) under drought stress. In this study, we investigated the role of *MeGRXC3* in regulating drought tolerance and corresponding downstream signalling in cassava. Our study provides new insight into the role of *MeGRXC3* in regulation of catalase activity in cassava under drought stress.

Results

MeGRXC3 is associated with the activity of catalase in cultivars of cassava under drought stress

There are 21 CC-type GRXs in cassava genome (Ruan *et al.,* 2018). *MeGRXC3* (*Manes.01G215000*) an intronless coding region that is 315 bp in length from 30 421 960 bp to 30 422 275 bp in cassava chromosome 1 (Figure 1a). We performed re-sequencing in 100 cultivars of cassava to investigate whether *MeGRXC3* is correlated with drought tolerance, and we investigated the association with drought-related marker-traits that we previously reported (Wang *et al.,* 2017). Re-sequencing of the genomic DNA of *MeGRXC3* revealed a total of 44 SNPs. Two SNPs in the promoter were significantly associated with drought tolerance coefficients (DTCs) of catalase activity in mature leaves at $P < 0.01$ (Figure 1b), suggesting that transcription of *MeGRXC3* is correlated with catalase activity in cassava cultivars under drought stress.

Under non-drought conditions, *MeGRXC3* was expressed weakly in leaf blades and strongly in petioles and trivially in roots (Figure 1c). Drought and ABA treatments led to up-regulation of *MeGRXC3* in leaf blades of cassava cultivar cv.60444 (Figure 1c). Moreover, expression of *MeGRXC3* was induced in mature leaves by drought in several cassava cultivars with differing genotypes (Figure 1d). Promoter activity analysis results revealed green fluorescence in leaf epidermal cells, including guard cells, of the *MeGRXC3Pro:MeGRXC3:GFP* transgenic *Arabidopsis* (Figure 1e, f). These indicate that *MeGRXC3* may be expressed in guard cells of cassava and play conserved roles across cultivars in response to drought.

MeGRXC3 negatively regulates tolerance to dehydration *in vitro* in transgenic cassava

Overexpression of *MeGRXC3* resulted in sensitivity to drought in transgenic *Arabidopsis* (Figure S1). Therefore, we produced transgenic plants overexpressing *MeGRXC3:GFP (MeGRXC3-OE)* or expressing *RNAi* against *MeGRXC3* (*MeGRXC3-RNAi*) in cv.60444. In total, we successfully generated 13 transgenic cassava lines (Figure S2). Thus, we used two independent lines of *MeGRXC3*-OE (OE#12, OE#88) and of *MeGRXC3*-RNAi (RNAi#1, RNAi#17) in subsequent experiments.

We observed no significant phenotypic differences among control plants comprising wild-type and transgenic *in vitro* plantlets after grew on cassava basic medium (CBM) for 50 days (Figure 2a). However, root development of all plantlets was strongly inhibited by polyethylene glycol (PEG; Figure 2a). Moreover, we found that only the OE plantlets showed dwarf phenotypes (Figure 2a). Under PEG treatment, biomass of the OE plantlets was lower than that of controls; a much greater effect than in the wild-type plantlets and RNAi plantlets. (Figure 2b). These data indicate that *MeGRXC3* negatively regulates tolerance to dehydration in cassava. The Western blot and green fluorescence in abaxial epidermal cells including guard cells suggest that the MeGRXC3:GFP protein complex is expressed in OE transgenic cassava (Figure 2c,d).

MeGRXC3 negatively regulates drought tolerance in transgenic cassava seedlings

Prior to drought treatment, there were no obvious phenotypic differences among 90-day-old seedlings of transgenic and wild-

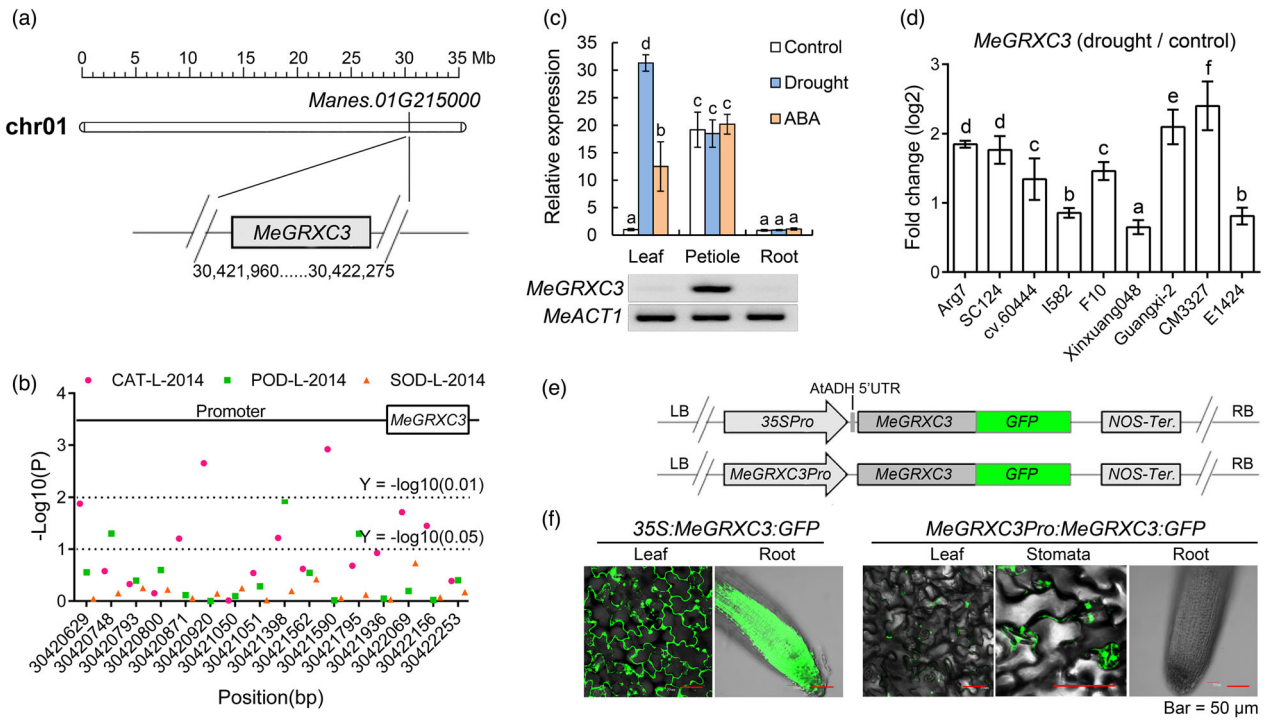

Figure 1 *MeGRXC3* is associated with catalase in cassava cultivars under drought stress. (a) A schematic diagram representing the *MeGRXC3* locus in the cassava genome. (b) SNPs in *MeGRXC3* genomic DNA are associated with drought trait coefficients of catalase (CAT-L-2014), peroxidase (POD-L-2014) and superoxide dismutase (SOD-L-2014) in 100 cultivated cassava germplasm under drought stress. (c) Expression analysis of *MeGRXC3* in cassava cv.60444. Upper panel: qPCR analysis of *MeGRXC3* in leaf, petiole and root under drought and ABA treatments. Bottom panel: RT-PCR of *MeGRXC3* in leaf, petiole and root of cassava cv.60444. Error bars are ±SD (n = 3). (d) qPCR analysis of *MeGRXC3* in leaves of different cultivated cassava under drought treatment. Expression levels of *MeGRXC3* were normalized against control plants. Error bars are ±SD (n = 3). (e) Schematic diagrams representing the design of the *35S:MeGRXC3:GFP* and *MeGRXC3Pro:MeGRXC3:GFP* constructs. (f) Analysis of the *MeGRXC3* promoter activity using transgenic *Arabidopsis*. Images show the fusion of the *MeGRXC3:GFP* construct protein in leaf and root tissues of *35S:MeGRXC3:GFP* transgenic *Arabidopsis* (left panel) and *MeGRXC3Pro:MeGRXC3:GFP* transgenic *Arabidopsis* (right panel). Different letters indicate differences with $P < 0.05$ (ANOVA test).

type cassava. At the time of 20 days drought treatment, we observed that the leaves and shoot apexes of the OE and wild-type cassava were withered, but the shoot apexes and several leaves of RNAi cassava remained alive (Figure 3a). After re-watering, plants grew under normal conditions for 7 days before we calculated their survival rates. After 7 days, only a few of OE and wild-type cassava seedlings were survived, while most RNAi cassava seedlings were survived (Figure 3b). These results support that *MeGRXC3* negatively regulates drought tolerance in transgenic cassava.

The transcript level of *MeGRXC3* in OE cassava leaves was much higher than that in wild-type cassava leaves (Figure 3c). Under drought stress, the expression of *MeGRXC3* was dramatically repressed by transgenes in RNAi cassava leaves (Figure 3c). qRT-PCR result showed that the *MeGRXC3*-RNAi transgenes had no effect on the expression of other drought-responsive CC-type GRXs under non-drought condition, and it did not alter their expression patterns under drought stress (Figure S3). Thus, the drought tolerance improvement of RNAi cassava can be explained by knock-down of *MeGRXC3*.

We performed stomatal assays by using six mature leaves of these cassava seedlings (Figure S4). Since MeGRXC3:GFP was predominantly localized in the nucleus of guard cells of OE transgenic cassava (Figure S5), stomatal movement assays of transgenic cassava seedlings help to clarify the functions of *MeGRXC3*. We classified stomatal status as open or closed upon examination by microscopy (Figure S5). Just before drought stress (i.e. 0 day drought treatment), the OE and RNAi plants showed no obvious differences in stomatal status (Figure 3d). After drought stressed for 6 days, most stomata of OE cassava, and half of the stomata of wild-type cassava were opened, while only a few stomata of the RNAi cassava were opened (Figure 3d). Further assays show that transpiration rates of leaves of the OE cassava were higher than that of the wild type (Figure 3e), while transpiration rates of leaves of the RNAi lines were lower than that of the wild type (Figure 3e). No significant difference in stomatal index was observed among the transgenic and wild-type leaves of cassava (Figure 3f). These data indicate that *MeGRXC3* negatively regulates drought-induced stomatal closure.

MeGRXC3 regulates expression of *MeCAT7* and distribution of drought-induced ROS in epidermal cells in cassava

Abscisic acid and jasmonic acid (JA) are important positive signalling hormones promoting stomatal closure. No obvious difference in endogenous ABA levels among all leaves of cassava was observed under non-drought and drought stress (Figure 4a). Under normal watering conditions, endogenous JA levels of transgenic cassava leaves were slightly lower than that of wild-type leaves (Figure 4b). However, we observed no differences in endogenous JA levels among treated cassava leaves at 6 days drought treatment (Figure 4b). Therefore, ABA and JA biosynthesis in transgenic

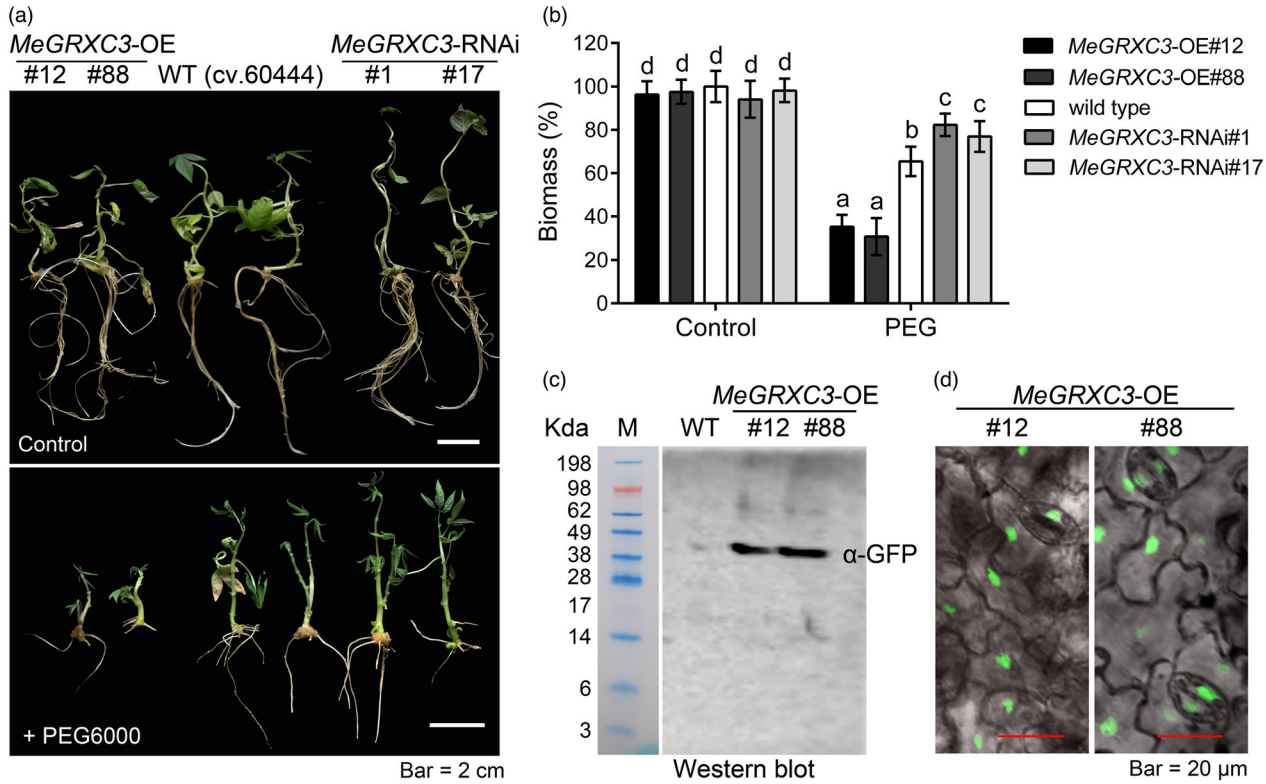

Figure 2 *MeGRXC3* transgene affects drought tolerance *in vitro* in cassava. (a) *in vitro* plantlets of transgenic and wild-type cassava (cv.60444) were grown on cassava basic medium (CBM) or on CBM containing 8% PEG6000. WT: wild type. (b) Analysis of biomass of transgenic cassava plantlets under PEG treatment. Biomass of wild-type cassava plantlets grown on CBM was set to 100%. Error bars are ±SD (n = 10). (c) Western blot of *MeGRXC3*-OE transgenic cassava lines #12 and #88. (d) Expression of *MeGRXC3:GFP* construct in epidermal peels of leaves of cassava representing *MeGRXC3*-OE. Green fluorescence indicating the localization of the *MeGRXC3:GFP* construct. Different letters indicate differences with $P < 0.05$ (ANOVA test).

cassava leaves under drought stress were not affected by *MeGRXC3* transgenes.

Compared with wild type, leaves of both the OE and RNAi cassava exhibited a higher base level of H_2O_2 under normal conditions (Figure 4c). We observed an increased H_2O_2 content in the RNAi and wild-type cassava leaves at 6 days drought treatment (Figure 4c). On the contrary, there was a slight decline in H_2O_2 content in the leaves of OE cassava at 6 days drought treatment. (Figure 4c). These findings indicate that *MeGRXC3* plays a role in response to drought by regulating H_2O_2 homeostasis in leaves of cassava.

Drought led to increased SOD activity in OE leaves of cassava but reduced it in RNAi and wild-type leaves (Figure 4d). Consistently, POD and CAT activities in both OE and RNAi cassava leaves were relatively lower than those in the wild type under normal watering conditions (Figure 4e,f). Reduced POD and CAT activities were detected in all of transgenic and wild-type cassava leaves at 6 days drought treatment (Figure 4e,f) but were much lower in the RNAi lines compared with the other two.

Our qRT-PCR analysis indicated that the relative expression level of *MeCAT1* and *MeCAT7* in the mature leaves of wild-type cassava was much higher than that of the other five *MeCAT*s under non-drought stress (Figure S6). Expression of *MeCAT1* was up-regulated in leaves of OE cassava, while it was down-regulated in leaves of RNAi cassava (Figure 4g). Both *MeGRXC3*-OE and -RNAi transgenic cassava did not affect drought-induced up-regulation of *MeCAT2* in leaves (Figure 4h). Under normal conditions, *MeCAT7* was down-regulated in leaves of OE cassava, while it was up-regulated in leaves of RNAi cassava (Figure 4i), and under drought conditions, RNAi plants maintained higher levels of *MeCAT7* than the wild-type and OE cassava (Figure 4i). Nevertheless, *MeGRXC3*-transgenic cassava did not alter drought-induced down-regulation of *MeCAT1* or *MeCAT7* in leaves. Taken together, these results suggest that

Figure 3 MeGRXC3 transgene affects drought tolerance of cassava seedling. (a) Drought treatment of transgenic and wild-type (WT) cassava (cv.60444) plants. D0: 0 day drought treatment; D10: 10-day drought treatment; D20: 20 day drought treatment; RW: re-watering; RW-7d: 7 day after re-watering. (b) Survival rates were reported following the drought treatment. Error bars are ±SD (n = 12). (c) qPCR analysis of *MeGRXC3* expression in drought-stressed leaves from transgenic and WT cassava plants. D6: 6-day drought treatment. Error bars are ±SD (n = 3). (d) Leaf abaxial surface showing difference in stomatal closure of the transgenic and WT cassava under drought conditions. Red arrow represents open stomata. (e) Transpiration rates of six mature leaves (4th, 5th, 6th, 7th, 8th and 9th from the apical bud) of the transgenic and WT cassava under normal conditions and drought stress. Black dot is mean of five leaves at the same position from the apical bud (n = 5). (f) Stomatal index of the six mature leaves from transgenic and WT cassava. Error bars are ±SD (n = 6). Different letters indicate differences with $P < 0.05$ (ANOVA test).

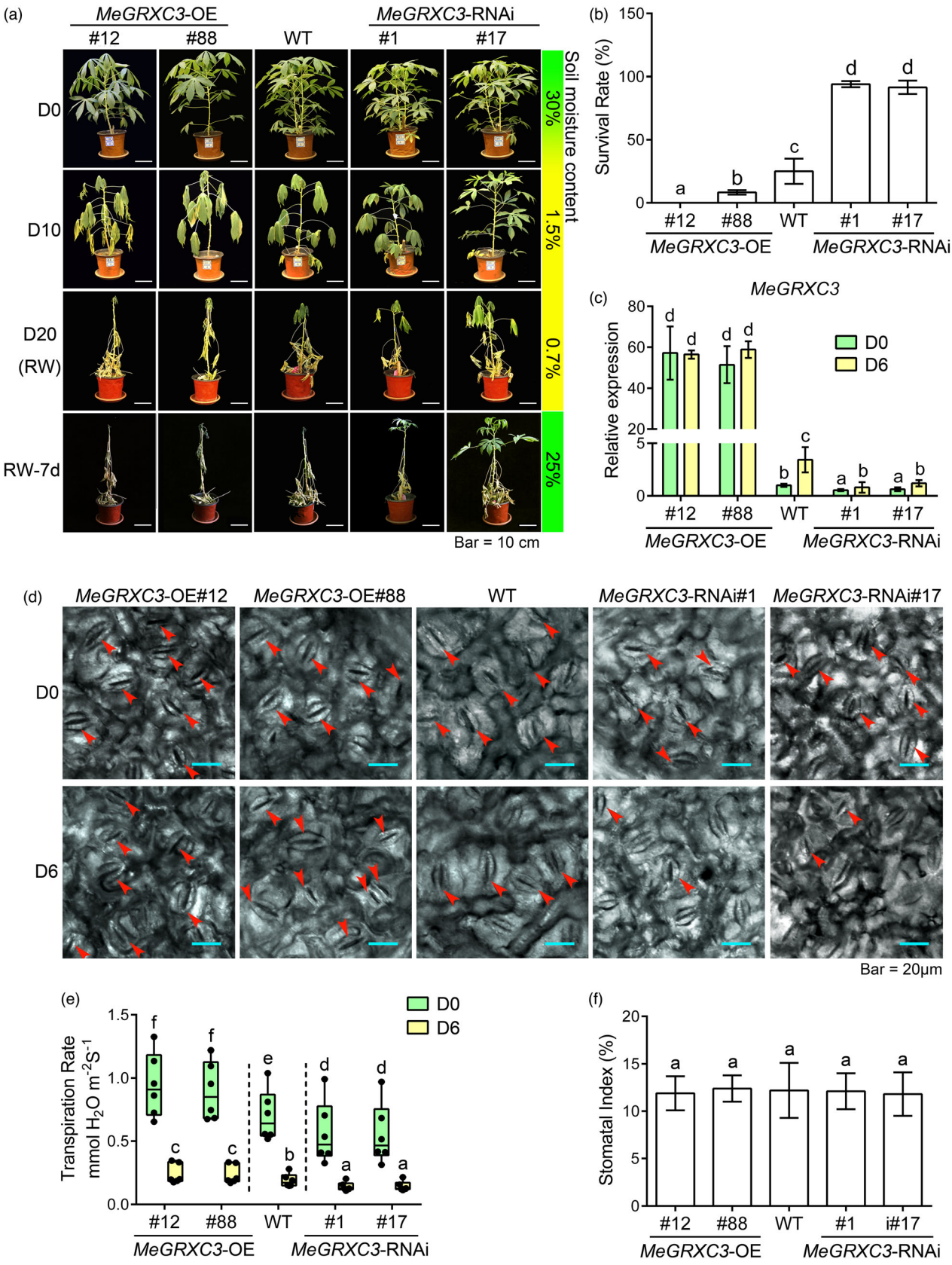

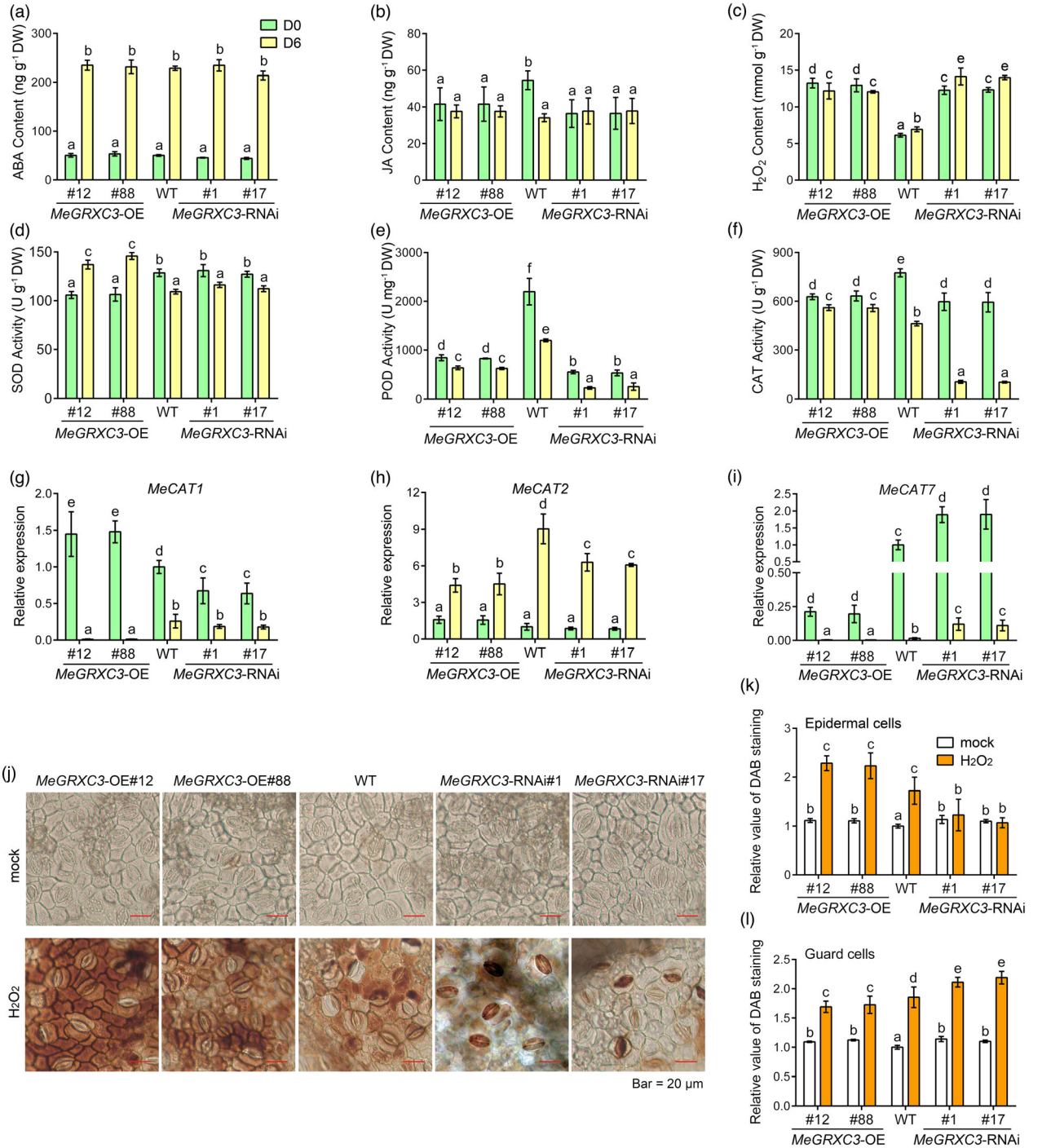

Figure 4 *MeGRXC3* transgene alters the expression of *MeCAT7* and distribution of drought-induced ROS in epidermal cells of cassava leaves. ABA content (a), JA content (b), H_2O_2 content (c), SOD activity (d), POD activity (e) and CAT activity (f) in mature leaves from transgenic and wild-type cassava under drought conditions. D0: 0 day drought treatment; D10: 10-day drought treatment. Error bars are ±SD (n = 3). The expression levels of *MeCAT1* (g), *MeCAT2* (h) and *MeCAT7* (i) in mature leaves of transgenic and wild-type cassava. Expression levels of these genes were normalized against that in wild-type plants before drought stress. Error bars are ±SD (n = 3). (j) DAB staining of abaxial epidermal cells and guard cells in mature leaves of cassava under H_2O_2 treatment. DBRW: day before re-watering. (k) Relative value of DAB staining in abaxial epidermal cells. Error bars are ±SD (n = 200). (l) Relative value of DAB staining in guard cells. Error bars are ±SD (n = 200). Different letters indicate differences with $P < 0.05$ (ANOVA test).

MeGRXC3 may regulate the expression of *CAT* genes in a complex manner in cassava in response to drought.

We stained H_2O_2 by DAB in abaxial epidermal cells of leaves of transgenic cassava after H_2O_2 treatment, and this revealed a build-up of H_2O_2, but it was distributed throughout the epidermis in the OE lines and predominantly in guard cells of the leaves of RNAi cassava (Figure 4j–l). These results indicate that *MeGRXC3* negatively regulates H_2O_2 accumulation in guard cells. *MeGRXC3*

transgenes negatively regulated water loss rate in leaves of cassava (Figure S7). This may partly explain the reduced drought tolerance in OE cassava and increased drought tolerance in RNAi cassava, as ABA-induced stomatal closure dependent on ROS signalling in *Arabidopsis* (Pei *et al.,* 2000). Our data indicate that *MeGRXC3* negatively regulates ABA-induced H_2O_2 accumulation in guard cells of cassava and, therefore, affects stomatal closure (Figure S7).

MeGRXC3 interacts with MeCAT1 and MeCAT2 to regulate the activity of catalase

The total soluble protein extract isolated from mature leaves of OE#88 cassava was checked by Western blot with anti-GFP antibody (Figure 5a, input). Proteins that immunoprecipitated with anti-GFP antibody were loaded in an SDS-PAGE gel (Figure 5a, IP). We identified IPed proteins by LC-MS/MS. From these IPed proteins (Data S1), we found three putative catalases comprising MeCAT1, MeCAT2 and MeCAT7 (Figure 5b), suggesting that MeGRXC3 probably interacts with catalases *in vivo*.

We screened MeCAT1 and MeCAT2, but not MeCAT7 by applying a MeGRXC3 non-transcriptional activation ability mutant, MeGRXC3P65L, as bait in the Y2H screening. Y2H assay indicates that MeGRXC3 interacts with MeCAT1 and MeCAT2 in yeast cells (Figure 5c). Green fluorescence was detected for co-expression of *MeGRXC3:NYFP/CYFP* and *MeCAT1:CYFP/NYFP*, or *MeCAT2:CYFP/NYFP* in bimolecular fluorescence complementation assay (BiFC) assay (Figure 5d). The outcomes showed that MeGRXC3 interacted with MeCAT1 and MeCAT2 in plant cells *in vivo*. We monitored catalase activity in tobacco leaves with transient co-expression of *MeGRXC3* and *MeCAT1*, or *MeCAT2*. The results showed that MeGRXC3 reduced catalase activity of MeCAT1 but enhanced that of MeCAT2 (Figure 5e).

MeGRXC3 interacts with MeTGA2, a cassava TGACG-BINDING FACTOR

CC-type GRXs can regulate nuclear gene expression through interaction with TGA factors (Li *et al.,* 2011; Ndamukong *et al.,* 2007; Zander *et al.,* 2012). Therefore, it may be unsurprising that our Y2H assays showed that the MeGRXC3 protein was able to interact with MeTGA2 in yeast (Figure 6a). Nuclear green fluorescence was detected for co-expression of *MeGRXC3:NYFP/CYFP* and *MeTGA2:CYFP/NYFP* in BiFC assay (Figure 6b). Green fluorescence was detected only in the nucleus for transient co-expression of *MeTGA2:GFP* and *MeHistone3:mCherry* tobacco (Figure 6b, bottom panel). These BiFC results further elucidate the interaction of MeGRXC3 with MeTGA2 in the nucleus.

Moreover, MeTGA2 shows transcription activation ability in yeast (Figure 6c). We also performed a DNA-affinity purification sequencing (DAP-seq) to identify targets of MeTGA2 in cassava (Data S2 and S3). The TGACG-motif most often occurred in the core sequence 5′-TGACGTCATCA-3′ and was the most frequently enriched in MeTGA2 targets (Figure 6d). For MeTGA2, the binding targets showed several transcription factors according to our annotations and encompassed the transcription factors ERF, MYB, including *MeMYB63* according to the analysis in DAP-seq, and WRKY (Figure 6e).

MeMYB63 positively regulates the expression of *MeCAT7* and activity of catalase

We found three AC-elements in the *MeCAT7* promoter (Figure 7a). One such AC-element (5′-ACCAAC-3′) is a target of MYB63, which is a R2R3-MYB transcription factor that act as a transcriptional activator of the lignin biosynthetic pathway in *Arabidopsis* (Zhou *et al.,* 2009). Yeast one-hybrid assay showed that MeMYB63 bound to the *MeCAT7* promoter and the AC-element with the sequence 5′-ACCACA-3′ (Figure 7b). MeMYB63 was predominantly localized in the nucleus and showed transcriptional activation ability in yeast (Figure 7c,d). The MeMYB63 protein was expressed in *E. coli* and purified by affinity (Figure 7e). As the Electrophoretic mobility shift assay (EMSA) result indicates, MeMYB63 can directly bind to the wild-type AC-element (P1) but not the mutated sequences (P1m; Figure 7f,g). Furthermore, MeMYB63 dramatically enhanced the transcriptional activity of the *MeCAT7* promoter based on a LUC/REN dual-luciferase report assay using *ProMeCAT7:pGreen0800-luc* as a reporter (Figure 7h,i). Moreover, we transiently overexpressed *MeMYB63* in leaves of cassava cv.60444 (Figure 7j). Consistently, the result suggests that *MeMYB63* promoted the expression of *MeCAT7* and catalase activity in the leaves (Figure 7k,l). Thus, it can be concluded that MeMYB63 is a direct transcriptional activator of *MeCAT7*.

MeMYB63 is negatively regulated by MeTGA2 in cassava through interaction with MeGRXC3

The expression of *MeMYB63* was negatively regulated by *MeGRXC3* in mature leaves of cassava (Figure 8a). A TGACG-motif (5′-TGATTACGTCA-3′) was identified in the *MeMYB63* promoter based on the MeTGA2 DAP-seq results (Figure 8b). The yeast one-hybrid assay shows MeTGA2 binding to the promoter of *MeMYB63* (Figure 8c). Furthermore, the MeTGA2 protein was expressed in *E. coli* and the purified (Figure 8d,e). We found MeTGA2 directly binding to P2 (containing the 5′-TGATTACGTCA-3′ motif) but not the P2m promoter fragment of *MeMYB63* (Figure 8f,g). Subsequently, LUC/REN dual-luciferase report assay showed that MeTGA2 did not affect the activity of the *MeMYB63* promoter without MeGRXC3, while MeGRXC3 could reduce the activity of the *MeMYB63* promoter without MeTGA2 (Figure 8h,i). Furthermore, the activity of the *MeMYB63* promoter was significantly reduced by co-expression of *MeTGA2* and *MeGRXC3* (Figure 8i). Together, these results suggest that MeGRXC3 negatively regulate the expression of *MeMYB63*, probably by interacting with MeTGA2.

Discussion

Functional characterization of drought-responsive CC-type GRXs in *Arabidopsis* provided criteria for choosing *MeGRXC3* as a candidate that should be further investigated in transgenic cassava (Ruan *et al.,* 2022). Furthermore, target re-sequencing and association mapping analyses revealed that the genetic variation of the *MeGRXC3* promoter was significantly associated with the drought-efficient trait of catalase activity in cassava cultivars under drought stress (Figure 1). Likewise, significant associations between genetic variation in a maize CC-type GRX *ZmGRXCC14* and drought tolerance were found at the seedling stage (Ding *et al.,* 2019a). Thus, taken together, CC-type GRXs may play important roles in regulating drought tolerance of crops. Herein, we demonstrated the function of *MeGRXC3* in regulating drought tolerance of cassava cultivar.

Glutaredoxins play antagonistic roles in regulating drought tolerance in plants (Guo *et al.,* 2010; Hu *et al.,* 2017). Overexpression of *MeGRXC3* caused hypersensitivity to mannitol-induced osmotic stress in transgenic *Arabidopsis* (Ruan

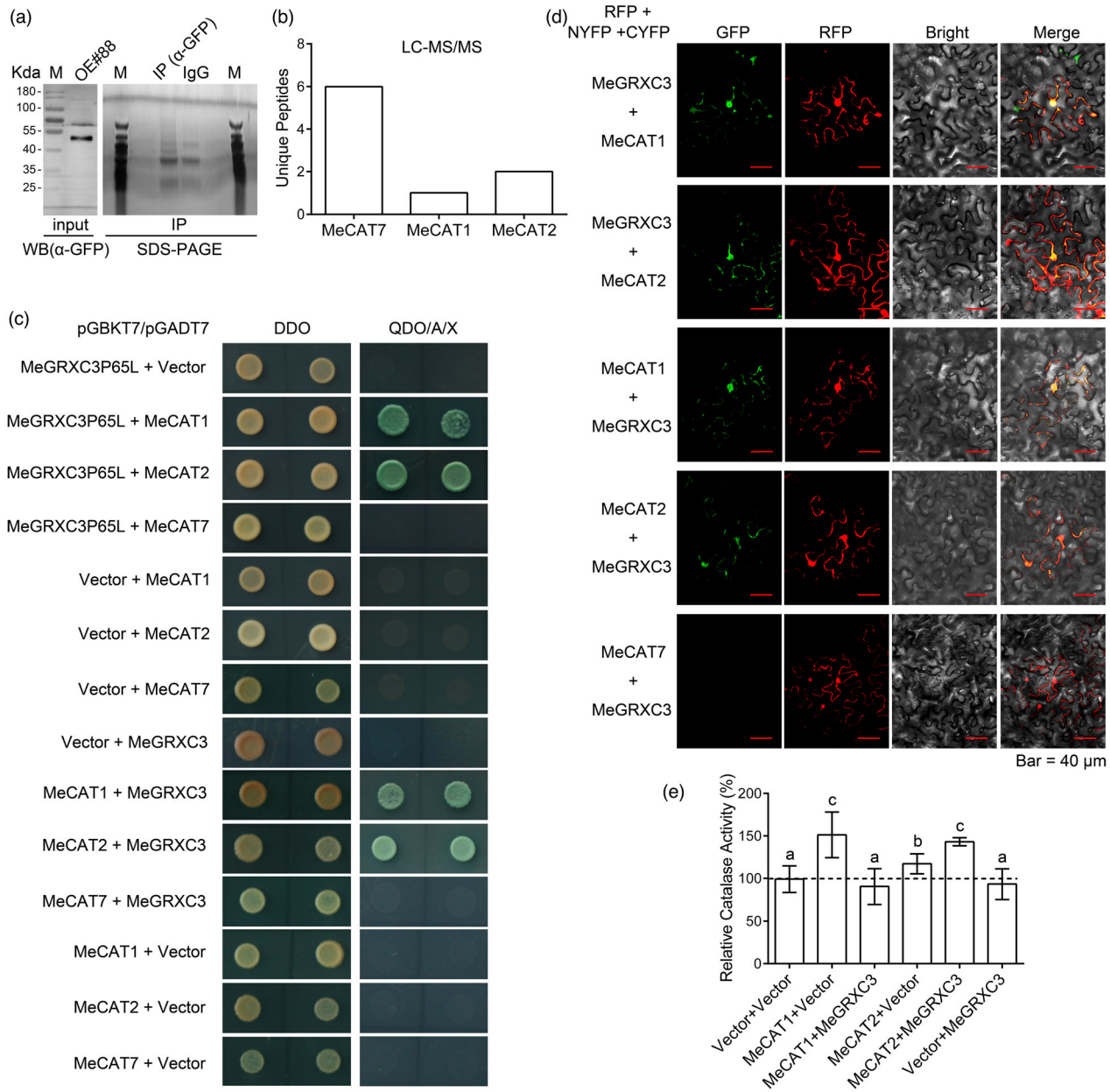

Figure 5 MeGRXC3 interacts with two catalases and regulates their activity. (a) Protein co-immunoprecipitation in MeGRXC3-OE transgenic cassava using Anti-GFP antibody. IP: immunoprecipitation. (b) Liquid chromatography–tandem mass spectrometry (LC-MS/MS) analysis of IPed proteins predicted three catalases as putative targets of MeGRXC3 in cassava. (c) MeGRXC3 interacts with MeCAT1 and MeCAT2 in yeast two-hybrid assay. (d) Bimolecular fluorescence complementation indicating the *in vivo* interaction of MeGRXC3 with MeCAT1 and MeCAT2 in tobacco leaves. Red fluorescence of mCherry was detected for colocalization analysis. (e) MeGRXC3 affects catalase activity of MeCAT1 and MeCAT2 in tobacco leaves. Relative catalase activity of tobacco that was co-transformed by two vectors (NYFP + CYFP) was set to 100%. Error bars are ±SD (n = 5), different letters indicate differences with $P < 0.05$ (ANOVA test).

et al., 2022), and conferred sensitivity to PEG and drought in transgenic *Arabidopsis* (Figure S1). In cassava, phenotypic analyses of *MeGRXC3* transgenic lines show that this gene negatively regulated PEG and drought tolerance (Figures 2 and 3). These data indicate that *MeGRXC3* acts as a negative regulator of drought tolerance in cassava. In fact, repression of *MeGRXC3* increased yield of tuber roots in the field in transgenic cassava under drought conditions (Figure S8a,b). Thus, *MeGRXC3* has agroeconomic potential for improving yield in cassava under drought stress. In addition, the dry matter rate of tuber roots from *MeGRXC3*-RNAi transgenic cassava is lower than that of wild type (Figure S8c), which may be because under drought stress, RNAi transgenic cassava has higher water use efficiency and therefore retain more water in its tuber root.

Glutaredoxin regulates stomatal movement by modulating ROS accumulation in guard cells in rice (Hu *et al.*, 2017). It remains

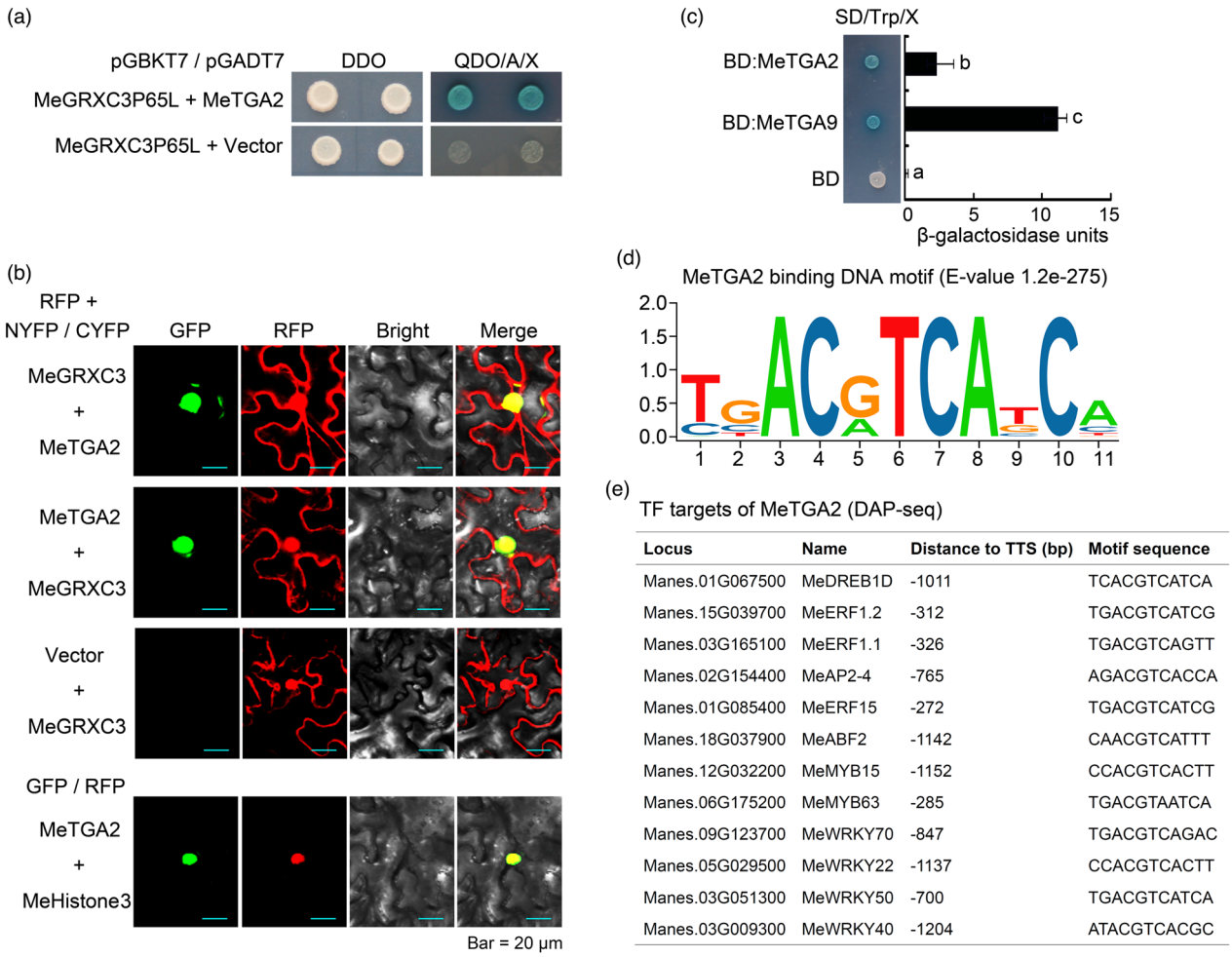

(e) TF targets of MeTGA2 (DAP-seq)

Locus	Name	Distance to TTS (bp)	Motif sequence
Manes.01G067500	MeDREB1D	-1011	TCACGTCATCA
Manes.15G039700	MeERF1.2	-312	TGACGTCATCG
Manes.03G165100	MeERF1.1	-326	TGACGTCAGTT
Manes.02G154400	MeAP2-4	-765	AGACGTCACCA
Manes.01G085400	MeERF15	-272	TGACGTCATCG
Manes.18G037900	MeABF2	-1142	CAACGTCATTT
Manes.12G032200	MeMYB15	-1152	CCACGTCACTT
Manes.06G175200	MeMYB63	-285	TGACGTAATCA
Manes.09G123700	MeWRKY70	-847	TGACGTCAGAC
Manes.05G029500	MeWRKY22	-1137	CCACGTCACTT
Manes.03G051300	MeWRKY50	-700	TGACGTCATCA
Manes.03G009300	MeWRKY40	-1204	ATACGTCACGC

Figure 6 MeGRXC3 interacts with a TGA transcription factor MeTGA2 in the nucleus. (a) MeGRXC3 interacts with MeTGA2 in yeast two-hybrid assay. (b) Bimolecular fluorescence complementation indicating the *in vivo* interaction of MeGRXC3 with MeTGA2 in tobacco leaves. Red fluorescence of mCherry was detected for colocalization analysis. For positive control, colocalization of *MeTGA2:GFP* and *MeHistone3:mCherry* constructs was detected. (c) Transcription activation analysis of MeTGA2 in yeast. Error bars are ±SD (n = 3). (d) Cassava DNA motifs bound by MeTGA2 in DNA-affinity purification sequencing (DAP-seq). The most abundant motif is shown. (e) Predicted transcription factor targets of the MeTGA2 in cassava based on the DAP-seq analysis. Different letters indicate differences with $P < 0.05$ (ANOVA test).

unclear whether the CC-type GRX can regulate stomatal movement in cassava. However, analysis of promoter activity indicates that *MeGRXC3* express in leaf epidermal cells including guard cells (Figure 1f), so we infer that *MeGRXC3* may be involved in regulation of stomatal movement. When the 35S promoter drove *MeGRXC3* to be expressed in guard cells in the *MeGRXC3*-OE lines, the MeGRXC3 protein was predominately localized in the nucleus of the transgenic cassava (Figures 2d and S5). Thus, stomatal movement assays of transgenic cassava can lend partial support to the function of *MeGRXC3* (Figure 3d), and the mechanism is likely by modulation of ROS accumulation in guard cells (Figure 4j–k). Stomatal movement assays revealed that the phenotypic changes in water loss rate in transgenic cassava can possibly be ascribed to impairment or enhancement of ABA-induced stomatal closure (Figure S7). It can be concluded that less water loss might be one of the main reasons to confer drought tolerance in *MeGRXC3*-RNAi transgenic cassava. In tropical regions, drought often occurs with high temperature, which may result in increased plants water absorption from the soil (Ogbonnaya *et al.*, 2017). Under drought and heat stress conditions in the field, greater drought tolerance of *MeGRXC3*-RNAi transgenic cassava may be associated with better chances of recovery when moisture stress is relieved. Our data provide a genetic engineering strategy to develop drought-resistant cassava varieties.

Both ABA and JA are important for stomatal movement (Kollist *et al.*, 2014; Zhu *et al.*, 2020), and ABA biosynthesis is essential for drought tolerance in cassava (Wei *et al.*, 2020). We found that the *MeGRXC3* transgene did not affect biosynthesis of ABA and JA in cassava under drought conditions (Figure 4a,b). In *Arabidopsis*, a CC-type GRX gene, *GRXS13*, was found to be able to negatively regulate base-level and oxidative stress-induced production of ROS (Laporte *et al.*, 2012). ROS production is often induced by ABA, and ROS and ABA operate in tandem as key signals involved in stomatal closure (Lee *et al.*, 2012; Yan *et al.*, 2007; Zhao *et al.*, 2016). Interestingly, in our study, base-level and drought-induced production of H_2O_2 in leaves was enhanced in both OE and RNAi plants (Figure 4c). However, the *MeGRXC3* transgene antagonistically regulated H_2O_2 accumulation in epidermal cells and guard cells (Figure 4j–l). Similar to

our RNAi plants, repression of *OsGRXS17* in rice promoted ABA-induced stomatal closure by modulating ROS accumulation in guard cells (Hu *et al.,* 2017). Our results suggest that *MeGRXC3* negatively regulates ABA-induced stomatal closure by modulating H_2O_2 accumulation in guard cells (Figure S7), but the main function of *MeGRXC3* in stomatal regulation seems to be not only to inhibit stomatal closing because, therefore, it would be contradictory for cassava to induce the expression of *MeGRXC3* under drought conditions. A possible explanation is that *MeGRXC3* is involved in negative feedback regulation involving ROS to balance photosynthesis under drought (i.e. maintaining some stomatal opening for CO_2 entry, even under drought).

MeGRXC3 negatively regulated the activity of catalase in leaves of cassava under drought stress (Figure 4f). Previous studies have demonstrated that catalase activity is essential for drought-induced ROS accumulation in cassava, and it can be regulated either at transcription or post-translation (Wei *et al.,* 2020; Xu *et al.,* 2013a; Yan *et al.,* 2021b). There are seven catalase genes present in the cassava genome, and the transcript level of *MeCAT7* is the highest in leaves of cassava (Figure S6). We found that *MeGRXC3* negatively regulated expression of *MeCAT7* (Figure 4i), suggesting that MeGRXC3 may regulate the activity of catalase at the transcription level. Furthermore, catalases have been identified as having possible interactions with GRX proteins in plants (Rouhier *et al.,* 2005). In fact, our work shows that MeGRXC3 interacts with MeCAT1 and MeCAT2 (Figure 5a–d) and antagonistically affects activity of these two catalases (Figure 5e). Our study implicates that MeGRXC3 can regulate catalase activity at both transcription and post-translation levels.

In *Arabidopsis*, the CAT3 Cys343Thr mutant displays increased catalase but decreased transnitrosylase activity, and the S-nitrosylation of Cys-343 is critical to the main activities of CAT3 as a transnitrosylase instead of a catalase (Chen *et al.,* 2020). Cys-343 is a unique and highly conserved residue in CAT3, which is Thr-343 in MeCAT1, MeCAT2 and MeCAT7 (Figure S9). GRX carries out deglutathionylation of Cys residue through binding with GSH, thus changing the redox state of its target proteins (Gutsche *et al.,* 2015). Although MeGRXC3 may regulate catalase activity of MeCAT1 and MeCAT2 at post-translation level, it remains to be determined whether MeGRXC3 regulates catalase activity by post-translation modification.

MeGRXC3:GFP transiently expressed in tobacco and overexpressed in transgenic *Arabidopsis* indicates that MeGRXC3 is localized to both the nucleus and cytoplasm (Figures 1f and S10). Surprisingly, MeGRXC3 is predominantly localized in the nucleus as indicated by *MeGRXC3*-OE transgenic cassava (Figures 2d and S5a). Nuclear activity is critical for the function of some CC-type GRXs in plants. For example, ROXY1 predominantly functions in the nucleus, regulates TGA transcription factors and was found to have both positive and negative activity during petal development in *Arabidopsis* (Li *et al.,* 2009). We have demonstrated that nuclear activity is required for the function of *MeGRXC3* during regulation of mannitol-induced osmotic stress in transgenic *Arabidopsis*, which is dependent on the interaction with TGA factors (Ruan *et al.,* 2022). In this study, a protein interaction assay indicated that MeGRXC3 interacted with MeTGA2 in the nucleus (Figure 6a,b). MeTGA2 is a typical TGA transcription factor, which binds to a TGACG-motif with the sequence 5′-TGACGTCATCA-3′ in cassava (Figure 6b–d). In *Arabidopsis*, ROXY19 suppresses *AtPDF1.2* transcription by interacting with TGA transcription factors (Ndamukong *et al.,* 2007). It indicated that CC-type GRX can regulate expression of transcription factor through interaction with TGA factors in plant. In prior studies, we also found that MeGRXC3 and MeGRXC15 can regulate expression of several stress-related transcription factors through interaction with TGA factors in transgenic *Arabidopsis* (Ruan *et al.,* 2018, 2022). Here, via DAP-seq, we identified several stress-related transcription factors as potential targets of MeTGA2 (Figure 6e), including MeDREB1D, which we reported previously (Yang *et al.,* 2016). In brief, together with quantitative real-time PCR (qPCR) results (Figure S11), our data indicate that MeGRXC3 may regulate the expression of these transcription factors by forming a transcriptional regulatory complex with MeTGA2 in the nucleus.

The regulation of *MeCAT7* by MeGRXC3 appears somewhat enigmatic. Specifically, the DAP-seq analysis revealed that *MeCAT7* is not a direct target of MeTGA2. Therefore, MeGRXC3 may regulate the expression of *MeCAT7* through other transcription factors. We did find three AC-elements, which could be bound by the transcription factors AtMYB61 and AtMYB63 (Prouse and Campbell, 2013; Romano *et al.,* 2012; Zhou *et al.,* 2009), in the promoter of *MeCAT7* (Figure 7a). *MeMYB63* was predicted as a putative target of MeTGA2 (Figure 6e), which could bind to the *MeCAT7* promoter and the AC-element in yeast and was identified as a transcription factor (Figure 7b–d). EMSA and dual LUC/REN reporter assays indicate that MeMYB63 directly bound to an AC-element in the *MeCAT7* promoter and positively regulated its activity (Figure 7f–h). Additionally, *MeMYB63* up-regulated transcription of *MeCAT7* and consequently promoted activity of catalase in cassava leaves (Figure 7i–l). These findings indicate that MeMYB63 is a transcriptional activator of MeCAT7.

Previous reports showed that *AtMYB61* is a positive regulator of stomatal closure (Liang *et al.,* 2005; Romero-Romero *et al.,* 2018). Whether *MeMYB63* is involved in stomatal movement in cassava merits further investigation. Nevertheless, this work taken together with prior studies suggests that *MeGRXC3* may regulate the expression of *MeCAT7* dependent

Figure 7 MeMYB63 directly binds to the *MeCAT7* promoter and initiates transcription of *MeCAT7*. (a) Schematic diagram represents AC-elements in the *MeCAT7* promoter. (b) MeMYB63 binding to MeCAT7 promoter and AC-elements in yeast one-hybrid assay. (c) Subcellular localization of MeMYB63 in tobacco leaves. Red fluorescence of the *MeHistone3:mCherry* construct was used as a nuclear localization reference. (d) Transcription activation analysis of MeMYB63 in yeast. (e) Expression of the SUMO-MeMB63 complex in bacteria (left) and purified SUMO-MeMB63 (right). Φ: negative control; M: protein marker; NPE: the soluble supernatant fraction; DPE: the supernatant of denatured protein; 1, 3: induced at 16 °C; 2, 4: induced at 37 °C. (f) Probes used in the electrophoretic mobility shift assay. (g) MeMYB63 binding to AC-elements in electrophoretic mobility shift assay. (h) Plasmids used in dual-luciferase reporter assay. (i) Relative luciferase (LUC/REN) activity of the *MeCAT7* promoter in tobacco leaves with transient expression of *MeMYB63*. Error bars are ±SD (n = 5). qPCR analysis of *MeMYB63* (j) and *MeCAT7* (k) in cassava leaves with transient expression of *MeMYB63*. Error bars are ±SD (n = 3). (l) Relative catalase activity in cassava leaves with transient expression of *MeMYB63*. Error bars are ±SD (n = 5). Different letters indicate differences with $P < 0.05$ (ANOVA test).

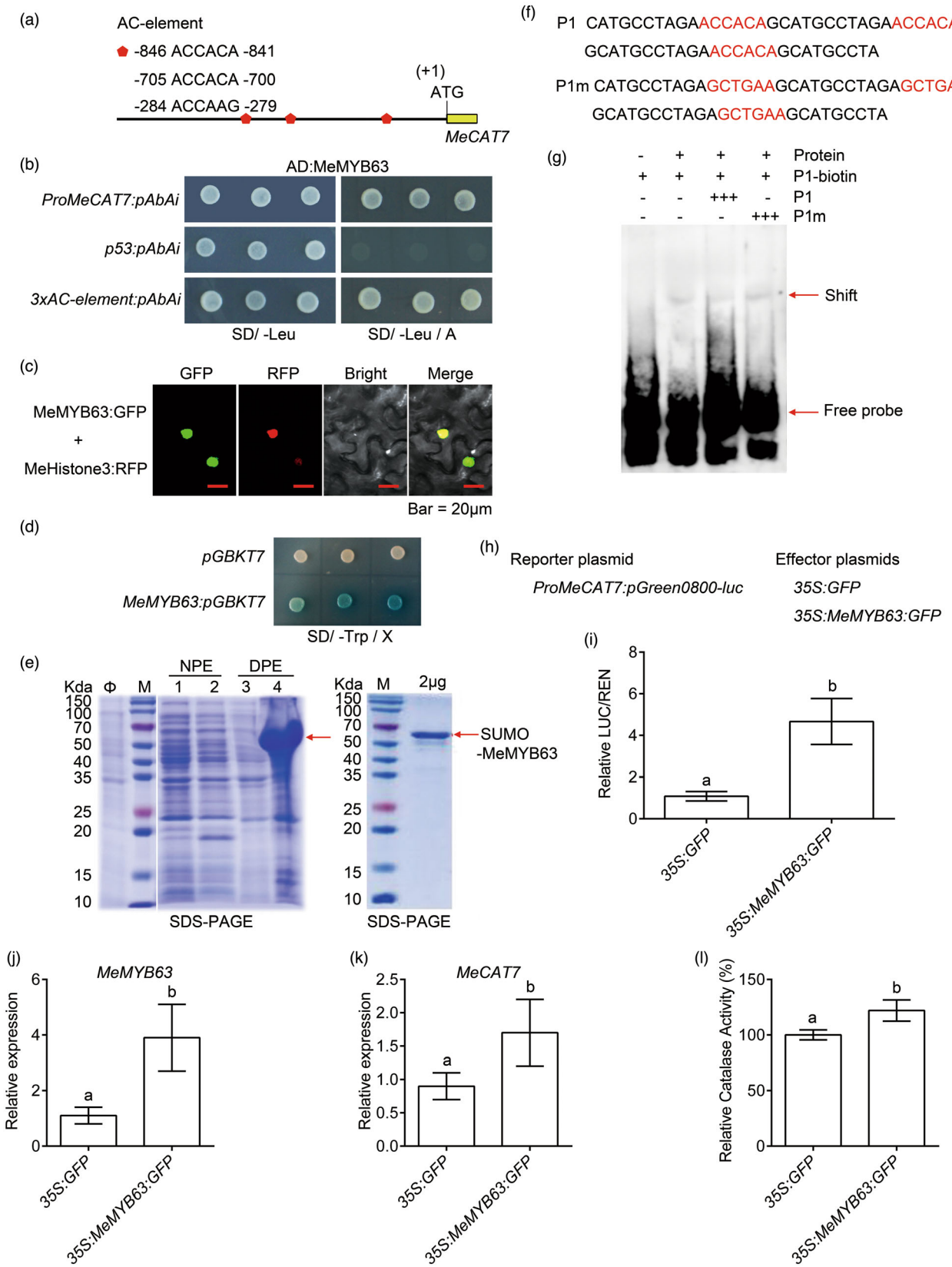

on *MeMYB63*. Here, we show that MeMYB63 in leaves of cassava was negatively regulated by *MeGRXC3* (Figure 8a), and that, when the TGACG-motif with the sequence 5′-TGATTACGTCA-3′ in the promoter of *MeMYB63* was bound by MeTGA2, the activity of *MeMYB63* promoter was diminished in the presence of MeTGA2 and MeGRXC3 (Figure 8b–i). Therefore, it can be logically (although tenuously) concluded that MeGRXC3 negatively regulates the expression of *MeCAT7*

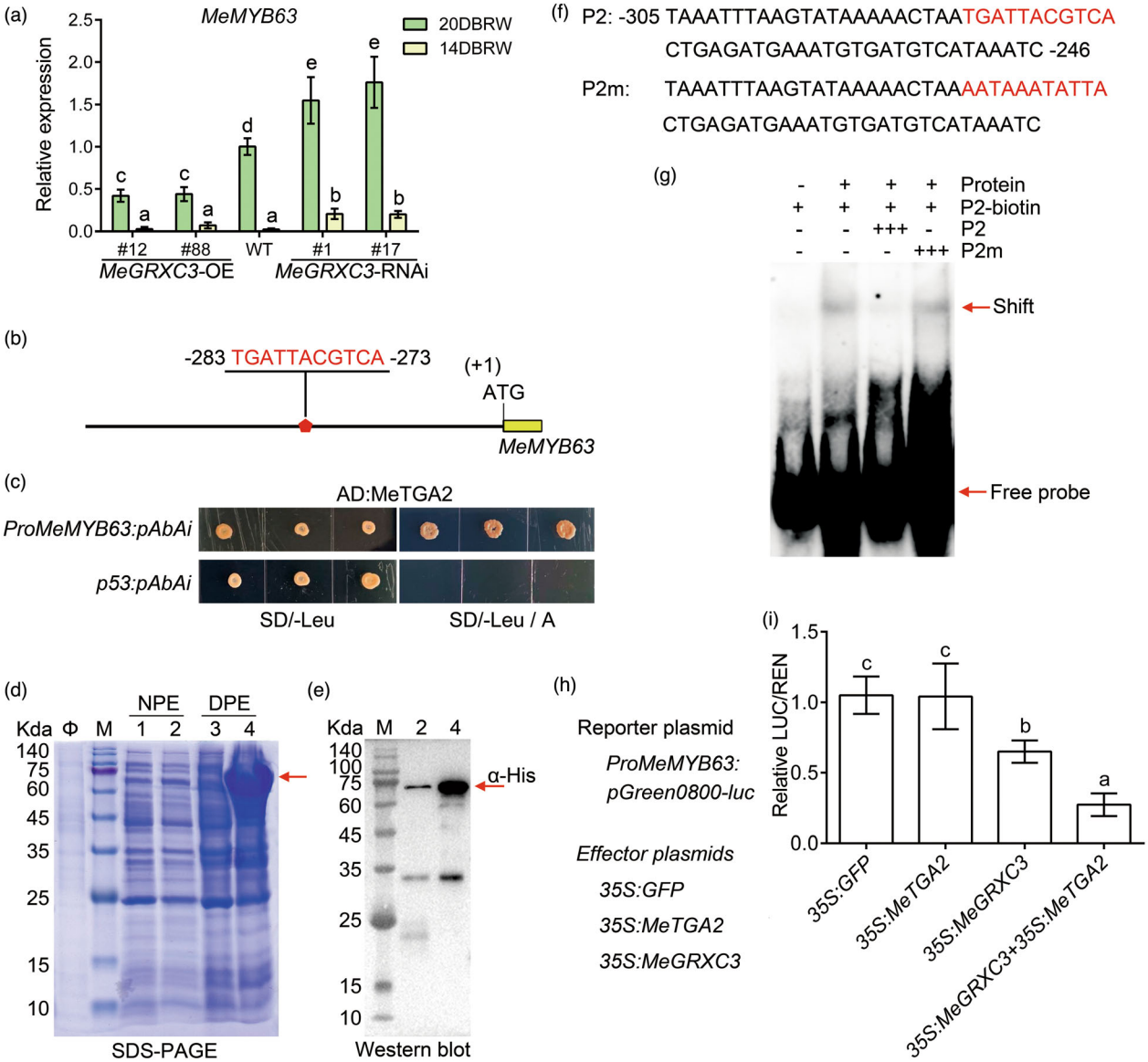

Figure 8 MeGRXC3-MeTGA2 complex acts as transcriptional repressor of *MeMYB63*. (a) qPCR analysis of *MeMYB63* in transgenic cassava under drought stress. Error bars are ±SD (n = 3). (b) Schematic diagram represents the TGACG-motif in the *MeMYB63* promoter. (c) MeTGA2 binding to the *MeMYB63* promoter in a yeast one-hybrid assay. (d) SUMO-MeTGA2 expression in bacteria. Φ: negative control; M: protein marker; NPE: the soluble supernatant fraction; DPE: the supernatant of the denatured protein; 1, 3: induction with IPTG at 16 °C; 2, 4: induction with IPTG at 37 °C. (e) Western bolt analysis of the purified SUMO-MeTGA2 protein complex. (f) Probes used in the electrophoretic mobility shift assay. (g) MeMYB63 binding to the TGACG-motif of the *MeMYB63* promoter in the electrophoretic mobility shift assay. (h) Plasmids used in a dual-luciferase reporter assay. (i) Relative luciferase (LUC/REN) activity of the *MeMYB63* promoter in tobacco leaves with transient expression of *MeGRXC3* and *MeTGA2*. Error bars are ±SD (n = 5). Different letters indicate differences with $P < 0.05$ (ANOVA test).

by repressing *MeMYB63* through interaction with MeTGA2 in cassava.

RNA-seq analysis indicated that MeGRXC3 regulates many drought-responsive genes, including a portion of transcription factors such as members of AP2/ERF, MYB and WRKY in cassava (Figure S12). Together, we summarized our study in a diagram of *MeGRXC3* associating with catalases and participating in cassava response to drought, which is shown in Figure 9. Our study expands the knowledge of CC-type GRX in plants and highlights the potential value of *MeGRXC3* for improvement of drought tolerance in cassava cultivars.

Experimental procedures

Candidate gene re-sequencing and association mapping

We isolated the genomic DNA sequence of *MeGRXC3* in cassava cultivar cv.60444 and identified it according to its locus in cassava genome (https://phytozome.jgi.doe.gov, *M. esculenta* v8.1). A total of 100 accessions of cassava were chose for re-sequencing from among cassava germplasm resources collected by our laboratory (Wang *et al.*, 2017). We designed primers covering the entire candidate genomic region to amplify the candidate segments (Data S4). SNPs were identified by alignment with the

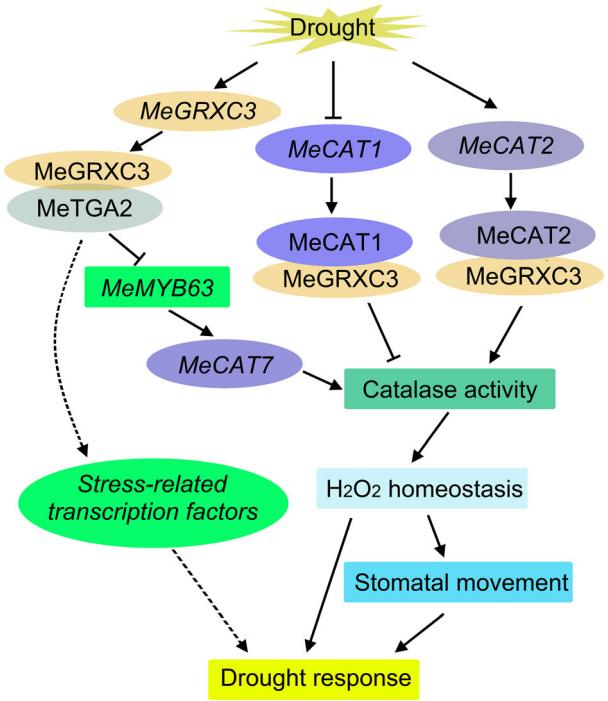

Figure 9 Proposed model of MeGRXC3 associating with catalases and modulating drought response in cassava.

MeGRXC3 genomic DNA sequence in the draft cassava genome (Data S5). The association mapping between SNPs and DTCs was performed as described in Appendix S1.

Plant materials and growth conditions

To study drought stress, stems of different cassava genotypes were cultured in pots for 90 days under greenhouse conditions (12 h/12 h of light/dark, 30 °C/25 °C day/night). The plants were kept in pots, which were 16 cm in diameter × 14 cm in height, containing well-mixed soil (soil : vermiculite : pellets, 1 : 1 : 1). We used cassava cultivar cv. 60444 as the wild type for this study because it can be used as a transgenic acceptor from cassava cultivars, and we produced transgenic cassava plants using this genotype as a background. For *Arabidopsis* plants for transformation, we used Col-0 as the wild type and grew plants under 12 h light/12 h dark at 20–23 °C until the primary inflorescences were 5–15 cm tall and a secondary inflorescence appeared at the rosette.

Drought treatment of cassava plants

For drought treatments, we treated eight different cassava cultivars, the wild type and transgenic cassava plants by water withholding. Continuously watered plants were used as controls. In each treatment, we used more than five plants of each line or genotype. We repeated the treatments twice for biological replication. After applying drought stress for 20 days, we re-watered all the treated wild type and transgenic plants. Following 7 days of normal watering, we determined survival rates. Throughout the experiment, we monitored soil moisture content of each pot using a moisture sensor once daily.

Quantitative real-time PCR

We isolated total RNA from tissues of cassava using an RNAprep Pure Plant Kit (TIANGEN, Beijing, China), and we synthesized cDNA with FastQuant RT Kits (TIANGEN). We performed gene expression analysis in cassava by qPCR with gene-specific primers (Data S4). All qPCR reactions were carried out in triplicate. To evaluate quantity of the amplified qPCR products, we used the comparative $\Delta\Delta C_T$ method.

Cassava transformation and molecular analysis of transgenic plants

We generated a hairpin RNA construct and a *35S:MeGRXC3phRNA* construct as per the method described in the reference (Ruan *et al.*, 2017). We transformed friable embryogenesis calluses of cassava cv.60444 using *Agrobacterium* strain LBA4404 carrying either DNA construct *35S:MeGRXC3:GFP* or *35S:MeGRXC3hpRNA*, and we selected transgenic cassava plants as previously described by Zainuddin *et al*. (2012). The transgenic cassava was identified by Southern blot and qPCR as in our previously reported (Ruan *et al.*, 2017). For identification of *MeGRXC3*-OE transgenic cassava, we performed Western blot by using anti-GFP as an antibody to detect the fused MeGRXC3:GFP protein. We imaged GFP fluorescence to identify subcellular localization of MeGRXC3 in the transgenic lines.

PEG treatments with transgenic cassava *in vitro* plantlets

For PEG treatment, we prepared two-layered media. The upper layer was a 3-cm-thick CBM, and the lower layer was either CBM (control) or CBM containing 8% PEG6000. We cut ~2 cm shoots of 40-day-old *in vitro* plantlets of wild-type and transgenic cassava plants and cultured them on the upper layer of the medium. Plantlets were cultured at 26 °C under 12-h light/12-h dark in a versatile environmental test chamber. After growing the plantlets for 50 days, we measured the weight of at least ten plantlets of each line to calculate biomass. Biomass of wild-type plantlets that grew in control medium was set to 100% in the assay.

Determination of stomatal conductance and rate of loss water

Using a microscope, we imaged the abaxial epidermises of mature leaves of cassava during drought stress, and we qualified stomata as being closed or open according to their aperture. We detected transpiration rate by Li-6400XT (LI-COR, Lincoln, NE) in six mature leaves (4th, 5th, 6th, 7th, 8th and 9th from the apical meristem). To calculate and average stomatal index, we used these six leaves from each line. For measurement of rate of water loss, we excised five mature leaves (5th, 6th, 7th, 8th and 9th from the apical meristem) from five unstressed transgenic or wild-type plants and kept them on plastic dishes at room temperature. We performed weight measurement at 2, 4, 8 and 24 h after excision. The rate of water loss was calculated by comparison with the initial fresh weight.

Determination of endogenous ABA and JA contents

We determined endogenous ABA and JA contents by extraction and detection using liquid chromatography electrospray ionization tandem mass spectrometry (LC-ESI-MS/MS) according to methods described previously (Ross *et al.*, 2004). We extracted 100 mg of mixed leaf sample with 1.5 mL of methanol formic acid solution (Methanol : formic acid : water = 7.8 : 0.2 : 2). Each sample comprised homogenized mature leaf tissue from three plants of each line as one biological replicate. We used three biological replicates for the results and a total of nine plants per line.

Determination of H_2O_2 quantity and enzyme assays

To measure the H_2O_2 content and SOD, POD and CAT activity in the mature leaves, we used the appropriate detection kit (H_2O_2 #BC3595; SOD #BC0175; POD #BC0195; CAT #BC0205, Solarbio, Beijing, China) following the manufacturer's instructions. Mature leaves from three plants of each line comprised one biological replicate. We used three biological replicates for the results and a total of nine plants per line.

Visualization of H_2O_2

H_2O_2 treatment of cassava leaves was performed as described in the reference (Xu *et al.,* 2013b). For cassava leaves, H_2O_2 was visualized by staining with diaminobenzidine (DAB) according to a widely accepted protocol. After infiltration with 2 mL of DAB solution (1 mg/mL DAB, pH 3.8) in an Eppendorf tube for 12 h, the leaves were immersed in 95% (w/v) boiling ethanol for 10 min to decolorize the chloroplasts. Epidermal peels from the abaxial surface of stained leaves were peeled off and imaged by a Zeiss Scope A1 Imaging System. The relative value of DAB staining in guard cells or epidermal cells was calculated using ImageJ. We performed calculations for at least 200 cells of each leaf.

For the ROS accumulation assay in guard cells of ABA-treated leaves, we infiltrated prepared epidermal peels with 50 μM 2,7-dichlorofluorescin diacetate (DCFH-DA) for 30 min. The resulting fluorescence was imaged by a confocal laser scanning microscope with excitation/emission at 488/515 nm. We calculated the fluorescent intensity from at least 50 guard cells of each leaf by FV10-ASW (Olympus, Tokyo, Japan).

Stomatal movement assay

We performed ABA-induced stomatal closing assays using mature leaves from cassava plants as previous reported (Sharma *et al.,* 2015) with slight modification. Prepared epidermal peels of the mature leaves were incubated in stomatal opening solution (10 mM KCl, 100 μM $CaCl_2$ and 10 mM MES, pH 6.1) for 12 h followed by incubation in stomatal opening solution supplemented with varying concentrations of ABA (0, 10, 50 and 100 μM) for eight more hours. We acquired photographs of stomata via an EVOS FL Imaging System and measured the stomatal aperture using the same software. We measured at least 200 stomata of each sampled mature leaf.

Immunoprecipitation and liquid chromatography and mass spectrometry (LC-MS/MS)

We extracted total protein from mature leaves of OE#88 transgenic cassava seedlings by IP lysis solution (#G2038, Servicebio, Wuhan, China). For input analysis, 40 μg of total protein was identified by Western blot using anti-GFP as an antibody. The protein complex was immunoprecipitated by anti-GFP and protein A/G-beads (#IP05, Millipore, Billerica, MA, USA). We checked the IPed protein complex by SDS-PAGE and digested by trypsin and then determined the precipitated fraction by LC-MS/MS (Data S1). We predicted candidate proteins by searching against the cassava protein database (https://www.uniprot.org; manihot esculenta.fasta).

Yeast two-hybrid assay (Y2H)

To screen for proteins potentially interacting with MeGRXC3, we performed a Y2H against a cDNA library of cassava mature leaves based on the Matchmaker Gold Yeast Two-Hybrid System User Manual using the DNA construct of *MeGRXC3P65L:pGBKT7* as bait. We introduced cDNA sequences of putative interacting proteins, *MeCAT1*, *MeCAT2*, *MeCAT7* and *MeTGA2*, into the *pGADT7* or *pGBKT7* expression vectors. These constructs were pairwise with *MeGRXC3P65L:pGBKT7/MeGRXC3:pGADT7* and co-transformed into yeast strain Y2HGold. We confirmed the presence of transformation by growth on DDO (SD/-Leu/-Trp) plates. We confirmed interactions between MeGRXC3 and MeCAT1/MeCAT2/MeTGA2 based on growth on QDO/X/A medium as described in the Y2H manual.

Bimolecular fluorescence complementation assay

To confirm the interactions between MeGRXC3 and MeCAT1/MeCAT2/MeCAT7, we performed a BIFC assay via a tobacco transient system as previously reported (Ruan *et al.,* 2018). The full-length coding sequence without the stop-codon of *MeGRXC3* was fused to the N- or C-terminus of yellow fluorescent protein (YFP) fragments (NYFP/CYFP) in frame to produce *35S:MeGRXC3:NYFP* and *35S:MeGRXC3:CYFP*. The full-length coding sequence without the stop-codon of *MeCAT1, MeCAT2, MeCAT7* and *MeTGA3* was fused in frame to CYFP or NYFP, respectively, to produce *35S:MeCAT1:CYFP*, *35S:MeCAT2:CYFP, 35S:MeCAT7:CYFP, 35S:MeTGA2:CYFP, 35S:MeCAT1:NYFP, 35S:MeCAT2:NYFP, 35S:MeCAT7:NYFP* and *35S:MeTGA2:NYFP*. The *35S:mCherry* (RFP) plasmid was used as a reference.

DNA-affinity purification sequencing

We performed DAP-seq binding assays as described previously (Bartlett *et al.,* 2017; O'Malley *et al.,* 2016) with modifications as described briefly by Yao *et al*. (2020). We used BLAST (Altschul *et al.,* 1990) against the cassava genome database (https://phytozome.jgi.doe.gov, *M. esculenta* v8.1) to identify potential target genes for annotation. Motifs were revealed using the MEME-ChIP suite 5.0.5 (Machanick and Bailey, 2011).

Electrophoretic mobility shift assay

The *MeMYB63* and *MeTGA2* were expressed in the Rosetta *Escherichia coli* strain. The protein extraction and purification were described in Appendix S1. Briefly, the supernatant comprises soluble (NPE) and denatured insoluble sediment (DPE) were determined by SDS-PAGE. Then, the MeMYB63 protein was qualified by SDS-PAGE, and MeTGA2 was checked by Western blot with anti-His as the antibody. We designed and labelled probes with biotin and mixed 2 μg of the purified protein MeMYB63 or MeTGA2 with the assigned probe at 25 °C for 20 min. We performed Western blot with Streptavidin-HRP Conjugate to detect the shift in bands.

Dual-luciferase (LUC/REN) reporter assay

We constructed reporter plasmids by cloning the *MeCAT7* and *MeMYB63* promoters into *pGreenII0800-luc* respectively to form *proMeCAT7:pGreenII0800-luc* and *proMeMYB63:pGreenII0800-luc*. For analysis of the *MeCAT7* promoter, the above-mentioned *35S:MeMYB63:GFP* was used as the effector, while *35S:MeTGA2:GFP* and *35S:MeGRXC3:GFP* were used as effectors in analysis of the *MeMYB63* promoter. We performed assays following the reference (Hellens *et al.,* 2005). The relative LUC/REN was analysed using the Dual-Luciferase Reporter Assay System (#0000469205, Madison, Promega, WI).

Statistical analyses

One-way ANOVA followed by Dunnett's multiple comparisons test was performed using GraphPad Prism version 6.00 for Windows (GraphPad Software, La Jolla CA, www.graphpad.com). In figures, different letters indicate significant differences of $P < 0.05$.

Accession numbers

Gene accession numbers were listed as follows: *MeGRXC3* (Manes.01G215000), *MeCAT1* (Manes.05G130500), *MeCAT2* (Manes.05G130700), *MeCAT4* (Manes.18G004500), *MeCAT7* (Manes.02G113300), *MeTGA2* (Manes.04G157200), *MeTGA9* (Manes.12G140100), *MeMYB63* (Manes.06G175200) and *MeHistone3* (Manes.13G097500). RNA-seq data from this study can be found in the GenBank/EMBL data libraries under following accession number: PRJNA797171.

Acknowledgements

We thank Dr. Bin Wang for association mapping. This work was supported by grants from the National Key R&D Program of China (2018YFD1000501), the Major Science and Technology plan of Hainan Province (ZDKJ2021012), the Central Public-interest Scientific Institution Basal Research Fund for the Chinese Academy of Tropical Agricultural Sciences (1630052022036) and Hainan Yazhou Bay Seed Lab (B21HJ0303). We appreciate the linguistic assistance provided by TopEdit (www.topeditsci.com) during the preparation of this manuscript.

Conflicts of interest

The authors declare there are no conflicts of interest.

Author contributions

MR planned and designed the research. MR, XG, XY, ZX, PZ, LZ and WL carried out the experiments. MR, XG, XY and MG performed data analyses. MR and XG wrote the manuscript. PZ, MP and MR revised the manuscript.

Data availability statement

The data that support the findings of this study are available in the supplementary material of this article.

References

Altschul, S.F., Gish, W., Miller, W., Myers, E.W. and Lipman, D.J. (1990) Basic local alignment search tool. *J. Mol. Biol.* **215**, 403–410.

Alves, A.A. and Setter, T.L. (2004) Response of cassava leaf area expansion to water deficit: cell proliferation, cell expansion and delayed development. *Ann. Bot.* **94**, 605–613.

Bartlett, A., O'Malley, R.C., Huang, S., Galli, M. and Ecker, J.R. (2017) Mapping genome-wide transcription-factor binding sites using DAP-seq. *Nat. Protoc.* **12**, 1659–1672.

Boyer, J.S. (1982) Plant productivity and environment. *Science*, **218**, 443–448.

Chen, L., Wu, R., Feng, J., Feng, T., Wang, C., Hu, J., Zhan, N. *et al.* (2020) Transnitrosylation mediated by the non-canonical catalase ROG1 regulates nitric oxide signaling in plants. *Dev. Cell*, **53**, 444–457.45.

Claeys, H. and Inze, D. (2013) The agony of choice: how plants balance growth and survival under water-limiting conditions. *Plant Physiol.* **162**, 1768–1779.

Ding, S., He, F., Tang, W., Du, H. and Wang, H. (2019a) Identification of maize CC-type glutaredoxins that are associated with response to drought stress. *Genes (Basel)*, **10**, 610.

Ding, Z., Wu, C., Tie, W., Yan, Y., He, G. and Hu, W. (2019b) Strand-specific RNA-seq based identification and functional prediction of lncRNAs in response to melatonin and simulated drought stresses in cassava. *Plant Physiol. Biochem.* **140**, 96–104.

El-Kereamy, A., Bi, Y.M., Mahmood, K., Ranathunge, K., Yaish, M.W., Nambara, E. and Rothstein, S.J. (2015) Overexpression of the CC-type glutaredoxin, OsGRX6 affects hormone and nitrogen status in rice plants. *Front. Plant Sci.* **6**, 934.

Guo, Y., Huang, C., Xie, Y., Song, F. and Zhou, X. (2010) A tomato glutaredoxin gene SlGRX1 regulates plant responses to oxidative, drought and salt stresses. *Planta*, **232**, 1499–1509.

Gutsche, N., Thurow, C., Zachgo, S. and Gatz, C. (2015) Plant-specific CC-type glutaredoxins: functions in developmental processes and stress responses. *Biol. Chem.* **396**, 495–509.

Hellens, R.P., Allan, A.C., Friel, E.N., Bolitho, K., Grafton, K., Templeton, M.D., Karunairetnam, S. *et al.* (2005) Transient expression vectors for functional genomics, quantification of promoter activity and RNA silencing in plants. *Plant Methods*, **1**, 13.

Hillocks, R.J., Thresh, J.M. and Bellotti, A. (2002) *Cassava: Biology, Production, and Utilization*. Wallingford, Oxon, UK, New York, NY: CABI Pub.

Hu, Y., Wu, Q., Peng, Z., Sprague, S.A., Wang, W., Park, J., Akhunov, E. *et al.* (2017) Silencing of OsGRXS17 in rice improves drought stress tolerance by modulating ROS accumulation and stomatal closure. *Sci. Rep.* **7**, 15950.

Kengkanna, J., Jakaew, P., Amawan, S., Busener, N., Bucksch, A. and Saengwilai, P. (2019) Phenotypic variation of cassava root traits and their responses to drought. *Appl. Plant Sci.* **7**, e01238.

Kollist, H., Nuhkat, M. and Roelfsema, M.R. (2014) Closing gaps: linking elements that control stomatal movement. *New Phytol.* **203**, 44–62.

Laporte, D., Olate, E., Salinas, P., Salazar, M., Jordana, X. and Holuigue, L. (2012) Glutaredoxin GRXS13 plays a key role in protection against photooxidative stress in Arabidopsis. *J. Exp. Bot.* **63**, 503–515.

Lee, S., Seo, P.J., Lee, H.J. and Park, C.M. (2012) A NAC transcription factor NTL4 promotes reactive oxygen species production during drought-induced leaf senescence in Arabidopsis. *Plant J.* **70**, 831–844.

Li, N., Muthreich, M., Huang, L.J., Thurow, C., Sun, T., Zhang, Y. and Gatz, C. (2019) TGACG-BINDING FACTORs (TGAs) and TGA-interacting CC-type glutaredoxins modulate hyponastic growth in *Arabidopsis thaliana*. *New Phytol.* **221**, 1906–1918.

Li, S., Gutsche, N. and Zachgo, S. (2011) The ROXY1 C-terminal L**LL motif is essential for the interaction with TGA transcription factors. *Plant Physiol.* **157**, 2056–2068.

Li, S., Lauri, A., Ziemann, M., Busch, A., Bhave, M. and Zachgo, S. (2009) Nuclear activity of ROXY1, a glutaredoxin interacting with TGA factors, is required for petal development in *Arabidopsis thaliana*. *Plant Cell*, **21**, 429–441.

Liang, Y.K., Dubos, C., Dodd, I.C., Holroyd, G.H., Hetherington, A.M. and Campbell, M.M. (2005) AtMYB61, an R2R3-MYB transcription factor controlling stomatal aperture in *Arabidopsis thaliana*. *Curr. Biol.* **15**, 1201–1206.

Liao, W., Wang, G., Li, Y., Wang, B., Zhang, P. and Peng, M. (2016) Reactive oxygen species regulate leaf pulvinus abscission zone cell separation in response to water-deficit stress in cassava. *Sci. Rep.* **6**, 21542.

Lindermayr, C., Sell, S., Muller, B., Leister, D. and Durner, J. (2010) Redox regulation of the NPR1-TGA1 system of *Arabidopsis thaliana* by nitric oxide. *Plant Cell*, **22**, 2894–2907.

Machanick, P. and Bailey, T.L. (2011) MEME-ChIP: motif analysis of large DNA datasets. *Bioinformatics*, **27**, 1696–1697.

Meyer, Y., Belin, C., Delorme-Hinoux, V., Reichheld, J.-P. and Riondet, C. (2012) Thioredoxin and glutaredoxin systems in plants: molecular mechanisms, crosstalks, and functional significance. *Antioxid. Redox Signal.* **17**, 1124–1160.

Murmu, J., Bush, M.J., DeLong, C., Li, S., Xu, M., Khan, M., Malcolmson, C. *et al.* (2010) Arabidopsis basic leucine-zipper transcription factors TGA9 and TGA10 interact with floral glutaredoxins ROXY1 and ROXY2 and are

redundantly required for anther development. *Plant Physiol.* **154**, 1492–1504.
Ndamukong, I., Abdallat, A.A., Thurow, C., Fode, B., Zander, M., Weigel, R. and Gatz, C. (2007) SA-inducible Arabidopsis glutaredoxin interacts with TGA factors and suppresses JA-responsive PDF1.2 transcription. *Plant J.* **50**, 128–139.
Ogbonnaya, F.C., Rasheed, A., Okechukwu, E.C., Jighly, A., Makdis, F., Wuletaw, T., Hagras, A. *et al*. (2017) Genome-wide association study for agronomic and physiological traits in spring wheat evaluated in a range of heat prone environments. *Theor. Appl. Genet.* **130**, 1819–1835.
O'Malley, R.C., Huang, S.C., Song, L., Lewsey, M.G., Bartlett, A., Nery, J.R., Galli, M. *et al*. (2016) Cistrome and epicistrome features shape the regulatory DNA landscape. *Cell*, **165**, 1280–1292.
Pei, Z.M., Murata, Y., Benning, G., Thomine, S., Klusener, B., Allen, G.J., Grill, E. *et al*. (2000) Calcium channels activated by hydrogen peroxide mediate abscisic acid signalling in guard cells. *Nature*, **406**, 731–734.
Prouse, M.B. and Campbell, M.M. (2013) Interactions between the R2R3-MYB transcription factor, AtMYB61, and target DNA binding sites. *PLoS ONE*, **8**, e65132.
Romano, J.M., Dubos, C., Prouse, M.B., Wilkins, O., Hong, H., Poole, M., Kang, K.Y. *et al*. (2012) AtMYB61, an R2R3-MYB transcription factor, functions as a pleiotropic regulator via a small gene network. *New Phytol.* **195**, 774–786.
Romero-Romero, J.L., Inostroza-Blancheteau, C., Orellana, D., Aquea, F., Reyes-Diaz, M., Gil, P.M., Matte, J.P. *et al*. (2018) Stomata regulation by tissue-specific expression of the *Citrus sinensis* MYB61 transcription factor improves water-use efficiency in Arabidopsis. *Plant Physiol. Biochem.* **130**, 54–60.
Ross, A.R., Ambrose, S.J., Cutler, A.J., Feurtado, J.A., Kermode, A.R., Nelson, K., Zhou, R. *et al*. (2004) Determination of endogenous and supplied deuterated abscisic acid in plant tissues by high-performance liquid chromatography-electrospray ionization tandem mass spectrometry with multiple reaction monitoring. *Anal. Biochem.* **329**, 324–333.
Rouhier, N., Villarejo, A., Srivastava, M., Gelhaye, E., Keech, O., Droux, M., Finkemeier, I. *et al*. (2005) Identification of plant glutaredoxin targets. *Antioxid. Redox Signal.* **7**, 919–929.
Ruan, M.B., Guo, X., Wang, B., Yang, Y.L., Li, W.Q., Yu, X.L., Zhang, P. *et al*. (2017) Genome-wide characterization and expression analysis enables identification of abiotic stress-responsive MYB transcription factors in cassava (*Manihot esculenta*). *J. Exp. Bot.* **68**, 3657–3672.
Ruan, M.B., Yang, Y.L., Li, K., Guo, X., Wang, B., Yu, X.L. and Peng, M. (2018) Identification and characterization of drought-responsive CC-type glutaredoxins from cassava cultivars reveals their involvement in ABA signalling. *BMC Plant Biol.* **18**, 329.
Ruan, M.B., Yu, X.L., Guo, X., Zhao, P.J. and Peng, M. (2022) Role of cassava CC-type glutaredoxin MeGRXC3 in regulating sensitivity to mannitol-induced osmotic stress dependent on its nuclear activity. *BMC Plant Biol.* **22**, 41.
Sharma, G., Giri, J. and Tyagi, A.K. (2015) Rice OsiSAP7 negatively regulates ABA stress signalling and imparts sensitivity to water-deficit stress in Arabidopsis. *Plant Sci.* **237**, 80–92.
Sharma, R., Priya, P. and Jain, M. (2013) Modified expression of an auxin-responsive rice CC-type glutaredoxin gene affects multiple abiotic stress responses. *Planta*, **238**, 871–884.
Suksamran, R., Saithong, T., Thammarongtham, C. and Kalapanulak, S. (2020) Genomic and transcriptomic analysis identified novel putative cassava lncRNAs involved in cold and drought stress. *Genes (Basel)*, **11**, 366.
Wang, B., Guo, X., Zhao, P., Ruan, M., Yu, X., Zou, L., Yang, Y. *et al*. (2017) Molecular diversity analysis, drought related marker-traits association mapping and discovery of excellent alleles for 100-day old plants by EST-SSRs in cassava germplasms (*Manihot esculenta* Cranz). *PLoS ONE*, **12**, e0177456.
Wang, Z., Xing, S., Birkenbihl, R.P. and Zachgo, S. (2009) Conserved functions of Arabidopsis and rice CC-type glutaredoxins in flower development and pathogen response. *Mol. Plant*, **2**, 323–335.
Wei, Y., Liu, W., Hu, W., Yan, Y. and Shi, H. (2020) The chaperone MeHSP90 recruits MeWRKY20 and MeCatalase1 to regulate drought stress resistance in cassava. *New Phytol.* **226**, 476–491.
Weng, X., Zhou, X., Xie, S., Gu, J. and Wang, Z.Y. (2021) Identification of cassava alternative splicing-related genes and functional characterization of MeSCL30 involvement in drought stress. *Plant Physiol. Biochem.* **160**, 130–142.
Wrzaczek, M., Brosche, M. and Kangasjarvi, J. (2013) ROS signaling loops – production, perception, regulation. *Curr. Opin. Plant Biol.* **16**, 575–582.
Xing, S. and Zachgo, S. (2008) ROXY1 and ROXY2, two Arabidopsis glutaredoxin genes, are required for anther development. *Plant J.* **53**, 790–801.
Xu, J., Duan, X., Yang, J., Beeching, J.R. and Zhang, P. (2013a) Coupled expression of Cu/Zn-superoxide dismutase and catalase in cassava improves tolerance against cold and drought stresses. *Plant Signal. Behav.* **8**, e24525.
Xu, J., Duan, X., Yang, J., Beeching, J.R. and Zhang, P. (2013b) Enhanced reactive oxygen species scavenging by overproduction of superoxide dismutase and catalase delays postharvest physiological deterioration of cassava storage roots. *Plant Physiol.* **161**, 1517–1528.
Yan, J., Tsuichihara, N., Etoh, T. and Iwai, S. (2007) Reactive oxygen species and nitric oxide are involved in ABA inhibition of stomatal opening. *Plant Cell Environ.* **30**, 1320–1325.
Yan, Y., Wang, P., Lu, Y., Bai, Y., Wei, Y., Liu, G. and Shi, H. (2021a) MeRAV5 promotes drought stress resistance in cassava by modulating hydrogen peroxide and lignin accumulation. *Plant J.* **107**, 847–860.
Yan, Y., Wang, P., Wei, Y., Bai, Y., Lu, Y., Zeng, H., Liu, G. *et al*. (2021b) The dual interplay of RAV5 in activating nitrate reductases and repressing catalase activity to improve disease resistance in cassava. *Plant Biotech. J.* **19**, 785–800.
Yang, Y., Liao, W., Yu, X., Wang, B., Peng, M. and Ruan, M. (2016) Overexpression of MeDREB1D confers tolerance to both drought and cold stresses in transgenic Arabidopsis. *Acta Physiol. Plant*, **38**, 243.
Yao, J., Shen, Z., Zhang, Y., Wu, X., Wang, J., Sa, G., Zhang, Y. *et al*. (2020) Populus euphratica WRKY1 binds the promoter of H+-ATPase gene to enhance gene expression and salt tolerance. *J. Exp. Bot.* **71**, 1527–1539.
Zainuddin, I.M., Schlegel, K., Gruissem, W. and Vanderschuren, H. (2012) Robust transformation procedure for the production of transgenic farmer-preferred cassava landraces. *Plant Methods*, **8**, 24.
Zander, M., Chen, S., Imkampe, J., Thurow, C. and Gatz, C. (2012) Repression of the *Arabidopsis thaliana* jasmonic acid/ethylene-induced defense pathway by TGA-interacting glutaredoxins depends on their C-terminal ALWL motif. *Mol. Plant*, **5**, 831–840.
Zhao, P., Liu, P., Shao, J., Li, C., Wang, B., Guo, X., Yan, B. *et al*. (2014) Analysis of different strategies adapted by two cassava cultivars in response to drought stress: ensuring survival or continuing growth. *J. Exp. Bot.* **66**, 1477–1488.
Zhao, Y., Chan, Z., Gao, J., Xing, L., Cao, M., Yu, C., Hu, Y. *et al*. (2016) ABA receptor PYL9 promotes drought resistance and leaf senescence. *Proc. Natl Acad. Sci. USA*, **113**, 1949–1954.
Zhou, J., Lee, C., Zhong, R. and Ye, Z.H. (2009) MYB58 and MYB63 are transcriptional activators of the lignin biosynthetic pathway during secondary cell wall formation in Arabidopsis. *Plant Cell*, **21**, 248–266.
Zhu, M., Geng, S., Chakravorty, D., Guan, Q., Chen, S. and Assmann, S.M. (2020) Metabolomics of red-light-induced stomatal opening in *Arabidopsis thaliana*: coupling with abscisic acid and jasmonic acid metabolism. *Plant J.* **101**, 1331–1348.

Supporting information

Additional supporting information may be found online in the Supporting Information section at the end of the article.

Figure S1 Overexpression of *MeGRXC3* confers PEG and drought sensitivity in transgenic *Arabidopsis*.
Figure S2 Molecular analysis of transgenic cassava.
Figure S3 Expression analysis of other drought-responsive CC-type GRXs in *MeGRXC3*-RNAi transgenic cassava.
Figure S4 Leaf positions of cassava seedling.
Figure S5 Cassava stomata.
Figure S6 Expression analysis of cassava catalase genes in mature leaf.
Figure S7 The *MeGRXC3* transgene affects ABA-induced stomatal closure.

Figure S8 Yield of tuber roots in the field in transgenic cassava under drought conditions.
Figure S9 Alignment of catalases from cassava and *Arabidopsis*.
Figure S10 Subcellular localization of MeCAT1, MeCAT2, MeCAT7, MeGRXC3 and MeHistone3.
Figure S11 qPCR analysis of six transcription factors in wild-type and transgenic cassava under drought conditions.
Figure S12 RNA-seq analysis of wild-type and transgenic cassava under drought conditions.
Appendix S1 Methods.

Data S1 Target proteins of MeGRXC3 identified by CoIP with LC-MS/MS in *MeGRXC3*-OE transgenic cassava.
Data S2 DAP-seq results of MeTGA2 in cassava.
Data S3 Candidate targets prediction of MeTGA2 based on DAP-seq analysis.
Data S4 Primers used in this study.
Data S5 SNPs in *MeGRXC3* genomic DNA.
Data S6 RNA-seq results of transcription factors, including AP2/ERF, MYB, TCP and WRKY in wild-type and transgenic cassava.

